538.54

ANOMALOUS PENETRATION OF ELECTROMAGNETIC FIELD IN A METAL AND RADIO-FREQUENCY SIZE EFFECTS

É. A. KANER and V. F. GANTMAKHER

Institute of Radiophysics and Electronics, Ukrainian Academy of Sciences;
Institute of Solid State Physics, USSR Academy of Sciences

Usp. Fiz. Nauk 94, 193–241 (February, 1968)

1. INTRODUCTION

IT is well known that under ordinary conditions the electromagnetic field does not penetrate deep into a metal and is localized in a thin layer near its surface. This phenomenon is called the skin effect. It is due to the large electric conductivity of metallic bodies: the external wave induces a high frequency electric current that prevents penetration of the field into the sample. The skin effect is characterized by a penetration depth and by a distribution of the field in the conductor. The penetration depth can be introduced in different manners, depending on the characteristic of the skin effect. In the classical (or normal) skin effect, which takes place at room temperatures, the field decreases exponentially. The penetration depth (the thickness of the skin layer) is usually defined as the distance δ_n in which the field decreases by a factor e. There is a well known formula for δ_n,

$$\delta_n = c(2\pi\omega\sigma_0)^{-1/2}, \tag{1.1}$$

where c is the speed of light, ω the circular frequency of the wave, and σ_0 the static conductivity of the metal. The change in the phase of the wave in the metal is characterized by the same quantity δ_n.

The definition (1.1) is directly connected with the law of distribution of the field inside the metal. It is possible to present a different definition of the thickness of the skin layer, which makes use of the external characteristic of the metal—its surface impedance $Z = R - iX$:

$$\delta_h = \frac{1}{H(0)}\int_0^\infty H(z)\,dz = \frac{ic^2}{4\pi\omega}Z = \frac{c^2}{4\pi\omega}(X - iR). \tag{1.2}$$

Here H(z) is one of the tangential components of the alternating magnetic field, and the z axis is directed along the inward normal to the surface of the sample. Such a definition of the penetration depth is more general, since it does not presuppose an exponential attenuation of the field in the skin layer. The exponential distribution takes place only in the case of the normal skin effect, when the mean free path l of the electron in the metal is much smaller than δ_n. Under these conditions, the quantity δ_h defined by (1.2) is connected with the δ_n by the relation $2\delta_h = \delta_n(1 + i)$.

In pure single crystals of metals at low temperatures, the mean free path l can reach values on the order of several millimeters. It is therefore easy to realize the opposite case, corresponding to the anomalous skin effect. In the anomalous skin effect, Ohm's law in its usual form $\mathbf{j} = \sigma\mathbf{E}$ no longer holds, since the current density $\mathbf{j}(\mathbf{r})$ at a given point $\mathbf{r}$ is determined by the electric field $\mathbf{E}$ not only at that point, but also in a region with dimension on the order of l around it. Consequently, the conductivity σ is not a constant of the metal, but depends on the form of the sample and on the field distribution in it, i.e., it is an integral operator. This operator should be determined from a microscopic theory. Such a theory was constructed by Reuter and Sondheimer[1] on the basis of a simultaneous solution of the kinetic equation for the distribution function of the electrons and of Maxwell's equations. It is shown in the cited paper that when $\delta_n \ll l$ the law governing the variation of the metal in the field is much more complicated than in the normal skin effect. For the anomalous skin effect, Re δ_h and Im δ_h determine only the order of magnitude of the rate of decrease of the amplitude and of the change of the phase of the electromagnetic field in the metal.

The dependence of δ_h on the frequency and on other quantities can be obtained with the aid of simple qualitative considerations, advanced to Pippard[2] and called in the literature the ineffectiveness concept. In the anomalous skin effect, not all the electrons are equivalent from the point of view of their role in the creation of the high frequency field. Those electrons which move at noticeable angles to the surface of the metal spend a relatively short time in the skin layer, and are then either scattered on the surface, or penetrate deep into the metal, where the electromagnetic field amplitude is small. Therefore the contribution of such electrons to the surface current is insignificant, and they are called "ineffective" electrons. The screening current is formed essentially by the "effective" electrons, which move at small angles to the surface and negotiate in the skin layer a distance on the order of the mean free path l. The effective electrons constitute a small fraction (on the order of $|\delta_h|/l$) of the total number of electrons, and therefore the conductivity produced by them is equal to $\sigma_{eff} = g\sigma_0\delta_h/l$, where g is a number on the order of unity. Substituting σ_{eff} for σ_0 in the formula for the impedance in the normal skin effect

$$Z = \left(\frac{4\pi\omega}{c^2\sigma_0}\right)^{1/2}\exp\left(-\frac{\pi i}{4}\right) \tag{1.3}$$

and using the definition (1.2), we get

$$\delta_h = \left(\frac{c^2 l}{4\pi g\omega\sigma_0}\right)^{1/3}\exp\left(-\frac{\pi i}{6}\right). \tag{1.4}$$

From a comparison with the exact formulas of[1] it follows that in the case of diffuse reflection $g = 2\pi/\sqrt{3}$.

Expressions (1.1) and (1.4) reflect the difference between the normal and anomalous skin effect. Whereas $\delta_n \sim \omega^{-1/2}$, the frequency dependence of δ_h is weaker, namely $\delta_h \sim \omega^{-1/3}$. In the anomalous skin effect, the

depth of the skin layer δ_h does not depend on the mean free path (and consequently on the temperature), since the ratio σ_0/l does not depend on l. Under the conditions of the normal skin effect we have $\delta_n \sim l^{-1/2}$. We shall henceforth make frequent use of the real quantity δ, which is of the same order as $|\delta_h|$. The exact expressions for δ will be given later in each individual case.

The dynamics of the conduction electrons in metals and the character of their interaction with the electromagnetic waves changes significantly in a constant magnetic field H. It has become clear in recent years that a metal in a magnetic field may turn out to be transparent to electromagnetic radiation, and in a number of cases it behaves in general like a dielectric.

All the presently known effects of anomalous penetration (AP) of the electromagnetic field into a metal can be subdivided into two groups. The first can be arbitrarily called the group of plasma or collective phenomena. They are due to the resonant excitation of collective motions of the electrons in the metal by an external wave. These collective oscillations represent weakly damped electromagnetic waves in the electron-hole plasma of the metal. From the point of view of the quasiparticle concept, such waves can be treated as secondary elementary excitations of the Bose type, occurring in a Fermi gas (or Fermi liquid) of primary excitations—electrons and holes. A detailed exposition of the properties of weakly damped waves in metals is contained in the review[3].

In the present review we consider AP effects of a different kind, those due to individual motion of charged quasiparticles in a magnetic field. The penetration of the electromagnetic field inside the metal is due to the electrons that "carry away" the high frequency field from the skin layers and then "reproduce" it within the volume of the metal. Such effects can be called penetration of the trajectory type. Unlike the case of excitation of collective oscillations, the frequency of the external field is no longer connected by the resonance conditions. The magnetic field intensity determines the scale of the picture of the distribution of the electromagnetic fields inside the metal. These effects were first pointed out by Azbel'[4], who considered one of the cases of AP of the trajectory type, namely, the occurrence of field peaks deep in a metal under cyclotron resonance conditions.

For the existence of AP effects of the trajectory type it is necessary to satisfy the conditions

$$\delta \ll D \lesssim l, \qquad (1.5)$$

where D is the characteristic dimension of the electron trajectories in the magnetic field. The right side of the inequality (1.5) is the criterion defining a strong magnetic field. The left side denotes that the skin effect should remain anomalous with respect to the characteristic dimension of the electron trajectory. The meaning of this condition is particularly easy to explain in terms of the ineffectiveness concept. The electron interacts most intensely with the electromagnetic field on those sections of the trajectory where it moves along the wave front, i.e., parallel to the surface of the metal: $v_z = 0$. The retardation of the field can be neglected, since the velocity of the electron v is usually much larger than the characteristic "phase velocity" $\omega\delta$ of the wave. The points $v_z = 0$ on the electron trajectory and the corresponding points on the orbits in p-space* will be called "effective". In view of the fact that in a magnetic field the velocity vector **v** changes on the trajectory, there exist, generally speaking, an infinite number of effective points. Satisfaction of the left side of inequality (1.5) signifies that some of these points are certainly located outside the skin layer. This is precisely the cause of the AP of the high-frequency field in the metal. When the electron moves along the effective section of the trajectory in the skin layer, it acquires a velocity increment $\Delta\mathbf{v}$. Consequently, it is the carrier of part of the skin current $\Delta\mathbf{j} = -e\Delta\mathbf{v}$ (e—absolute value of the electron charge). The vector $\Delta\mathbf{v}$ varies along the trajectory. At the next effective point, which is located deep inside the metal, the electron again moves parallel to the surface of the metal and produces increments to the velocity $\Delta\mathbf{v}$ and the current $\Delta\mathbf{j}$. The occurrence of a current parallel to the surface deep inside the sample is indeed a manifestation of the AP of the field in the metal, namely, current and field peaks are produced inside the metal, and the distances between them are determined by the dimensions of the electron trajectories.

The mechanism of the AP of the field depends on the type of trajectory. If the trajectory is closed, then the appearance of a peak can be expected in the plane z = D, where D is the dimension of the trajectory in the z-axis direction (Fig. 1). The peak is the "skin layer" for electrons whose trajectory is displaced a distance D into the metal. These electrons produce in turn the next peak at a depth 2D, etc. As a result, a unique "chain of trajectories" is produced, along which the electromagnetic field penetrates to large depths inside the metal.

In the case of an open trajectory with a non-zero average velocity component $\bar{v}_z$, a different mechanism of AP of the field is possible. The system of peaks is determined not by a chain of trajectories of different electrons, but by the trajectory of the electrons that drift deep into the metal directly from its surface (Fig. 2). The high-frequency current is localized near the planes $z = u_n$, where u_n is the depth of the n-th effective point (we assume that one of them is located on the surface z = 0).

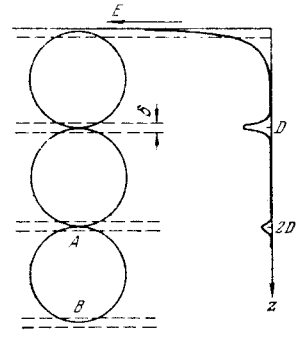

FIG. 1.

*To avoid confusion we point out that we are using the term "trajectory" when we are dealing with a motion of an electron in r-space, and "orbit" when we describe motions in momentum space.

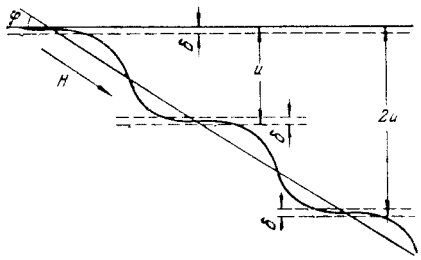

FIG. 2.

So far we have considered the motion of an individual electron. Actually there exist in the metal electrons that move along different trajectories with different values of D or u_n, which are functions of p_H—the projection of the momentum on the direction of the magnetic field H. For this reason, the secondary current is distributed, generally speaking, over a large depth. As a result of the averaging over all the electrons, the trajectories that are singled out are those for which the density of states with given values of D or u_n becomes infinite, i.e., electrons with extremal values $D(p_H) = D_{ext}$ or $u_n(p_H) = u_{ext}$. A relatively large number of effective electrons are focused at corresponding distances from the surface of the metal, and this ensures the occurrence of the peaks. The widths of the peaks are determined by the thickness of the skin layer, and to a much lesser degree by the distances between them. The field in the interval between the peaks is much weaker, although it differs from zero.

The AP of the field in a metal can be due also to ineffective trajectories. Then the spatial distribution of the field in the metal has a harmonic character.

We shall discuss below different mechanisms of focusing of effective electrons, and we shall present a classification of all the presently known cases of trajectory-type AP of the electromagnetic field in a metal. The first part of the present review is devoted to an exposition of the results of the theoretical investigation of field AP in a semi-infinite metal. A discussion of methods and results of the experimental study of AP is given in the second part. These methods are directly connected with a group of phenomena known as the radio frequency size effects[5].

2. Classification of Electron Trajectories

An important role in AP phenomena of the trajectory type is played by the shape of the electron trajectory. It is therefore, useful to recall the main features of the motion of a charged quasiparticle with an arbitrary dispersion law in a constant magnetic field (see[6]), and also to classify the different types of trajectories.

From the equations of motion

$$\dot{\mathbf{p}} = -\frac{e}{c}[\mathbf{vH}], \quad \dot{\mathbf{r}} \equiv \mathbf{v} = \frac{\partial \varepsilon}{\partial \mathbf{p}} \qquad (2.1)^*$$

it follows that the orbits of an electron are determined in momentum space by the integrals of motion

$$\varepsilon = \text{const}, \quad p_H = \frac{\mathbf{pH}}{H} = \text{const}. \qquad (2.2)$$

Geometrically, these orbits are the intersections of the equal-energy surface $\epsilon(p) = \text{const}$ and the planes $p_H = \text{const}$. Depending on the topology of the Fermi surface $\epsilon(p) = \epsilon_F$, the direction of the field H, and the values of p_H, the orbits can be either closed or open, i.e., they can pass continuously through the entire reciprocal lattice.

Since $\dot{\mathbf{p}}$ is the velocity of the electron in momentum space and v is the velocity in r space, it follows from (2.1) that the orbit in p-space and the projection of the trajectory of the electron on the plane perpendicular to H in r-space are similar, with a similarity coefficient eH/c, and are turned by $\pi/2$ relative to each other. The mean values of the electron velocity component along the magnetic field is determined by the formula

$$\bar{v}_H = -\frac{1}{2\pi m}\frac{\partial S(\varepsilon, p_H)}{\partial p_H}, \quad m = \frac{1}{2\pi}\frac{\partial S(\varepsilon, p_H)}{\partial \varepsilon}, \qquad (2.3)$$

where m is the effective mass of the electron and $S(\epsilon, p_H)$ is the area bounded by the plane curve (2.2). Using these data, we can easily classify the possible types of trajectories in r-space.

1. **Closed trajectories.** Inasmuch as $\bar{v}_H$ should vanish on these trajectories, it follows from (2.3) that these trajectories correspond to the intersections of (2.2) with the extremal surface S_{ext}. From symmetry considerations it is clear that on the open Fermi surface the trajectories of the central section $p_H = 0$ are always closed. We note that closed trajectories, generally speaking, are not plane curves.

2. **Helical trajectories.** These are obtained from non-central sections of the Fermi surface and are strictly periodic in r-space. The average electron velocity $\bar{\mathbf{v}}$ is parallel to H and depends on p_H.

3. **Trajectories of the vicinity of the elliptical limiting point.** The limiting point is defined as the point p_0 on the Fermi surface $\epsilon(p) = \epsilon_F$ at which the plane perpendicular to H is tangent to the surface and the orbit degenerates into a point. For all p_H close to p_0, the electron trajectories have the form of strongly elongated helical lines with practically equal pitch. On these orbits the cyclotron frequency $\Omega = eH/mc$ and the effective mass m are also practically the same.*

4. **Open trajectories.** These exist only in a metal with an open Fermi surface. The motion of the electron is infinite in a plane perpendicular to H. The average velocity $\bar{\mathbf{v}}$, generally speaking, has an arbitrary direction relative to the vector H.

I. THEORY

3. System of Equations

To develop the theory of AP of an electromagnetic field in a metal, it is necessary to solve Maxwell's equations. For a monochromatic wave ($\sim \exp(-i\omega t)$) in a half-space, these equations are of the form (we neglect the displacement current)

$$E_\alpha''(z) = -4\pi i\omega c^{-2} j_\alpha(z), \quad \alpha = x, y, \qquad (3.1)$$

$$j_z(z) = 0. \qquad (3.2)$$

*[vH] ≡ v × H.

*There can exist also hyperbolic and parabolic limiting points, but in such points the effective mass m and the cyclotron period $2\pi/\Omega$ become infinite. Therefore the corresponding trajectories do not lead to AP of the field in a metal.

The z axis is directed along the inward normal to the surface of the metal, and the y axis coincides with the projection of the vector H on the plane z = 0; E(z) and j(z) are the vectors of the electric field intensity and the current density, and the primes denote derivatives with respect to z. Equation (3.2) is the consequence of the continuity equation and is identical with the condition for electric quasineutrality of the metal.

To obtain the connection between j and E, we shall use the kinetic equation. In the approximation linear in the electric field, we have

$$-i\omega f + v_z \frac{\partial f}{\partial z} + \Omega \frac{\partial f}{\partial \tau} + \nu f = e\mathbf{E}\mathbf{v} \frac{\partial f_0}{\partial \varepsilon}, \tag{3.3}$$

$$\mathbf{j} = -\frac{2e}{(2\pi\hbar)^3} \int \mathbf{v} f \, d^3p; \tag{3.4}$$

here f is the non-equilibrium addition to the Fermi distribution function

$$f_0(\varepsilon) = \left[\exp\left(\frac{\varepsilon - \varepsilon_F}{T}\right) + 1\right]^{-1}, \tag{3.5}$$

$\tau = \Omega t$ is the dimensionless time (phase) of the motion of the electron along the orbit (2.2) in p-space, T is the temperature in energy units, and $2\pi\hbar$ is Planck's constant. In (3.3) we replaced the collision integral by the constant ν, which represents the frequency of the collisions of the electrons with the scatterers. The validity of introducing the collision frequency $\nu(p)$ in the anom0 alous skin effect is proved in[7].

The system (3.1)—(3.4) must be supplemented by the boundary conditions. When $z \to \infty$, all the functions vanish. On the surface z = 0 the tangential components of the electric and magnetic fields are continuous. For the function f we assume the diffuse-scattering condition

$$f\big|_{\substack{z=0,\\ v_z>0}} = 0. \tag{3.6}$$

As shown in[8,9], the solution of (3.3) is of the form

$$f(z, \tau, \varepsilon, p_H) = \frac{e}{\Omega(\varepsilon, p_H)} \frac{\partial f_0}{\partial \varepsilon} \int_{s(z,\tau,\varepsilon,p_H)}^{\tau} d\tau' \mathbf{v}(\tau', \varepsilon, p_H)$$

$$\times \mathbf{E}\left(z - \frac{1}{\Omega(\varepsilon, p_H)} \int_{\tau}^{\tau'} d\tau'' v_z(\tau'')\right) \exp\{(\nu - i\omega)(\tau' - \tau)\Omega^{-1}(\varepsilon, p_H)\}. \tag{3.7}$$

The function $s(z, \tau, \epsilon, p_H)$ takes into account the fact that the trajectory on which the electron has entered into the phase-space point (z, τ, ϵ, p_H) can start on the surface z = 0. In this case the function s is defined as the root of the equation

$$\Omega z + \int_{\tau}^{s} d\tau'' v_z = 0 \tag{3.8}$$

lying closest to τ and satisfying the condition $s \leq \tau$. If there is no such root (the electron "arrives" from inside the metal), then $s(z, \tau, \epsilon, p_H)$ should be set equal to $-\infty$ (for details see[8,9]).

Substituting (3.7) in (3.4), we get

$$j_i(z) = \frac{2e^2}{(2\pi\hbar)^3} \int_0^{\infty} d\varepsilon \left(-\frac{\partial f_0}{\partial \varepsilon}\right) \oint \frac{m\, dp_H}{\Omega} \int_0^{2\pi} d\tau v_i(\tau) \int_s^{\tau} d\tau' v_k(\tau')$$

$$\times \exp\left[\frac{\nu - i\omega}{\Omega}(\tau' - \tau)\right] E_k\left(z + \frac{1}{\Omega} \int_{\tau}^{\tau'} d\tau'' v_z(\tau'')\right). \tag{3.9}$$

An analysis shows that in all the cases discussed below the field component E_z in (3.9) can be neglected, and Eq. (3.2) can be completely disregarded. The problem thus reduces to a simultaneous solution of (3.1) and (3.9). This system of equations is particularly complicated in those cases when it is necessary to take into account the collisions of the electrons with the surface. In particular, collisions with the surface play an important role in field AP phenomena in the presence of drift motion of the effective electrons to the interior of the metal. The method of solving the system of equations (3.1) and (3.9) in such cases is discussed in Sec. 5.2.

On the other hand, it is shown in a number of papers that in AP phenomena due to the motion of effective electrons on closed trajectories (cyclotron resonance[7,4], field AP along a chain of trajectories[4,10], etc) it is possible to neglect the contribution of the electrons that collide with the surface. This means that in expressions (3.7) and (3.9) we can put $s = -\infty$ for all z, τ, ϵ, and p_H, i.e., we can use the electron distribution function for an unbounded metal. In this case, the electrodynamic problem in a half-space can be replaced by the simpler problem of finding the distribution of the high-frequency field in an unbounded medium.

We continue the functions $E_\alpha(z)$ in even fashion to the region $z < 0$ and change over to Fourier components

$$\mathcal{E}_\alpha(k) = 2\int_0^{\infty} dz E_\alpha(z) \cos kz, \qquad E_\alpha(z) = \frac{1}{\pi} \int_0^{\infty} dk \mathcal{E}_\alpha(k) \cos kz. \tag{3.10}$$

Substituting (3.10) in (3.9), we obtain a linear connection between the Fourier components $j_\alpha(k)$ and $\mathcal{E}_\beta(k)$ (α, β = x, y):

$$j_\alpha(k) = \sigma_{\alpha\beta}(k) \mathcal{E}_\beta(k), \tag{3.11}$$

where $\sigma_{\alpha\beta}(k)$ are the Fourier components of the two-dimensional conductivity tensor

$$\sigma_{\alpha\beta}(k) = \frac{2e^2}{(2\pi\hbar)^3} \int_0^{\infty} d\varepsilon \left(-\frac{\partial f_0}{\partial \varepsilon}\right) \oint \frac{m\, dp_H}{\Omega} \int_0^{2\pi} d\tau v_\alpha(\tau) \int_{-\infty}^{\tau} d\tau' v_\beta(\tau')$$

$$\times \exp\left[\frac{\nu - i\omega}{\Omega}(\tau' - \tau)\right] \cos\left(\frac{k}{\Omega} \int_{\tau}^{\tau'} d\tau'' v_z(\tau'')\right). \tag{3.12}$$

Equations (3.1) have in the Fourier representation the form

$$k^2 \mathcal{E}_\alpha(k) + 2E'_\alpha(0) = 4\pi i\omega c^{-2} \sigma_{\alpha\beta}(k) \mathcal{E}_\beta(k). \tag{3.13}$$

Hence

$$E_\alpha(z) = -2\pi^{-1} T_{\alpha\beta}(z) E'_\beta(0), \tag{3.14}$$

$$T_{\alpha\beta}(z) = \int_0^{\infty} dk \cos kz \, [k^2 \hat{I} - 4\pi i\omega c^{-2} \hat{\sigma}(k)]^{-1}_{\alpha\beta}, \tag{3.15}$$

where $\hat{I}$ is a unit matrix and $\hat{\sigma}(k)$ is the conductivity tensor (3.12). Formulas (3.14) and (3.15) yield the general solution of the problem of the distribution of the field in a metal in the case under consideration.

The physical meaning of such a method of solution lies in the fact that we represent the highly inhomogeneous field near the surface of the metal in the form of a superposition of plane monochromatic waves (expansion in a Fourier integral). The Fourier component of the connectivity tensor $\hat{\sigma}(k)$ describes the interaction of the conduction electrons with one of the harmonics of the wave packet. The integral effect of the interaction of the electrons with all the harmonics is determined by the inverse Fourier transformation (3.14) and (3.15). It is thus sufficient to limit oneself to an investigation of

the propagation of plane monochromatic waves $\mathscr{E}_\alpha(\kappa)\cos kz\exp(-i\omega t)$ in a metal. For this purpose it is necessary to determine the components of the tensor $\sigma_{\alpha\beta}(k)$.

One of the most important characteristics of a metal is the high-frequency surface-impedance tensor

$$Z_{\alpha\beta} = R_{\alpha\beta} - iX_{\alpha\beta}, \tag{3.16}$$

which is a generalization of the definition (1.2). The tensor $Z_{\alpha\beta}$ connects the values of the electric field on the surface with the tangential components of the total current $J_\alpha = \int_0^\infty dz j_\alpha(x)$:

$$E_\alpha(0) = Z_{\alpha\beta}J_\beta. \tag{3.17}$$

From (3.1) and from (3.14) and (3.15) it follows that

$$Z_{\alpha\beta} = -8i\omega c^{-2}T_{\alpha\beta}(0), \tag{3.18}$$

so that the field distribution and the impedance tensor are fully defined by the quantities $T_{\alpha\beta}(z)$.

We shall henceforth consider essentially the case of low frequencies

$$\omega \ll \nu, \tag{3.19}$$

when the quantity ω in (3.12) can be neglected. This means that the alternating field can be regarded as quasistatic, and its time variation produces only a skin layer in a metal.

4. Anomalous Penetration of a Field in a Metal Along a Chain of Trajectories

4.1. Chain of trajectories in a magnetic field parallel to the surface of the metal. In Sec. 1 we already mentioned the mechanism of field AP along a chain of trajectories. It is now necessary for us to ascertain the conditions for the occurrence of the peaks, the law governing the decrease of their intensity with increasing depth, and the factors that determine the widths of the individual peaks. We start with the simplest model, with which it is possible to illustrate the features of AP along a chain of trajectories[10]. We assume that the metal has a cylindrical Fermi surface $p_x^2 + p_y^2 = p^2$ = const, and that the magnetic field H is parallel to the y axis (the z axis is directed as before along the inward normal to the surface of the metal). This model is the simplest because all the electron trajectories are the same and represent circles of diameter D = 2pc/eH.

Let us calculate the elements of the transverse conductivity tensor $\sigma_{\alpha\beta}(k)$. It is obvious from symmetry considerations that only the element $\sigma_{xx}(k) \equiv \sigma(k)$ differs from zero. Assuming that $v_x(\tau) = v\cos\tau$, we obtain from (3.9)

$$\sigma(k) = \sigma_0\{|J^2_{1+i\gamma}(kR)| - \mathrm{Re}\,J_{1+i\gamma}(kR)J_{-1+i\gamma}(kR)\}, \tag{4.1}$$

$$\sigma_0 = \frac{e^2}{2}\left(\frac{v^2}{\nu}\frac{dN}{d\epsilon}\right)_{\epsilon_F}, \quad \gamma = \frac{\nu}{\Omega} \ll 1; \tag{4.2}$$

here σ_0 is the static conductivity, $dN/d\epsilon$ is the density of the electron states per unit energy interval, $N(\epsilon)$ is the electron density, R = D/2 is the radius of the electron trajectory in the magnetic field, and $J_\mu(z)$ is a Bessel function. In the model employed by us, the quantities ν, R, and Ω do not depend on p_H. Using the symptotic expression for the Bessel function at large values of the argument, we obtain

$$\sigma(k) = \frac{4\sigma_0}{\pi}\frac{\mathrm{ch}\,\pi\gamma - \sin kD}{kD}. \tag{4.3}$$

It is seen from this formula that the quantity $\sigma(k)$ can have deep minima when $\gamma \ll 1$: if kD = 2π(n + 1/4) (n—integer), then $\sigma \sim \sigma_0\gamma^2/kD$ and is much smaller than the mean value. The sharp decrease of $\sigma(k)$ is due to the fact that there are only two effective points, A and B, on the electron trajectories (see Fig. 1). When the diameter D spans an integer number of wavelengths, the resultant interaction of the electron with a given wave is small as a result of interference, for in one of these points the electron moves along the field, and in the other against the field. If the diameter spans an odd number of half-waves, the interaction is a maximum. The sharp decrease of $\sigma(k)$ when k = 2(n + 1/4)/D denotes a decrease of the absorption, as a result of which the wave penetrates deep into the metal to a large distance. Since the spectrum of the wave numbers of such penetrating waves is discrete and equidistant, a periodic system of narrow peaks is produced inside the volume of the metal. Their spatial width is determined by the number of the interfering components, i.e., in final analysis, by the depth δ of the skin layer. These arguments are confirmed by a rigorous calculation.

Let us investigate the function T(z), which describes the field distribution in the metal. Substituting (4.3) in (3.15), we get

$$T(z) = D\int_0^\infty \frac{dqq\cos qzD^{-1}}{q^3 - iM^3(\mathrm{ch}\,\pi\gamma - \sin q)}, \tag{4.4}$$

$$M = \frac{D}{\delta} \gg 1, \quad \delta = \left(\frac{c^2D}{16\omega\sigma_0}\right)^{1/3}. \tag{4.5}$$

Let us transform (4.4) in the following manner:

$$T(z) = D\sum_{s=0}^{\infty}\int_{2\pi s}^{2\pi(s+1)} dq \ldots = D\sum_{s=0}^{\infty}\int_0^{2\pi}\frac{dq'\,(2\pi s + q')\cos(2\pi s + q')zD^{-1}}{(2\pi s + q')^3 - iM^3(\mathrm{ch}\,\pi\gamma - \sin q')}. \tag{4.6}$$

We consider first the case z = nD. An important role in the sum over s is played by large values of s, on the order of $M/2\pi$. Therefore the quantity q' in the terms of the type $2\pi s + q'$ can be neglected, and the sum over s can be replaced by an integral. Calculating this integral, we get

$$T(nD) = \delta\exp\left(\frac{\pi i}{6}\right)\frac{2\pi}{\sqrt{27}}t_\gamma(n). \tag{4.7}$$

The function

$$t_\gamma(n) = \frac{1}{2\pi}\int_0^{2\pi}\frac{dq'\cos nq'}{(\mathrm{ch}\,\pi\gamma - \sin q')^{1/3}} \tag{4.8}$$

determines the decrease of the amplitude of the singularities with increasing number n. An analysis shows that for the first peaks ($n < 1/\pi\gamma$, i.e., $z < l$), the quantity γ in (4.8) can be set equal to zero and

$$t_\gamma(n) = t_\gamma(0)\cos\frac{n\pi}{2}\frac{\Gamma\left(n+\frac{1}{3}\right)\Gamma\left(\frac{2}{3}\right)}{\Gamma\left(n+\frac{2}{3}\right)} \sim \frac{\cos\frac{n\pi}{2}}{n^{1/3}},$$

$$t_\gamma(0) = \frac{2^{1/3}3^{1/2}\Gamma^2\left(\frac{1}{3}\right)}{2\pi\Gamma\left(\frac{2}{3}\right)} \simeq 1.85. \tag{4.9}$$

Thus, owing to the presence of the peaks, the surface

impedance Z turns out to be larger by a factor $t_\gamma(0)$ = 1.85 than the value of Z which would be obtained with that allowance for the AP of the field in the metal.

The more remote peaks (at depths $z > l$) decrease exponentially:

$$t_\gamma(n) = \frac{\cos\frac{n\pi}{2}}{\Gamma\left(\frac{1}{3}\right)} \frac{\exp(-n\pi\gamma)}{(n^2\pi\gamma)^{1/3}}. \quad (4.10)$$

It is easy to show that the field has a much smaller value far from the points z = nD. To this end we represent (4.6) in the form

$$T(z) = D\int_0^{2\pi} dq' \int_0^{\infty} \frac{ds 2\pi s \cos\left(2\pi s\zeta + \frac{z}{D}q'\right)}{(2\pi s)^3 - iM^3(\mathrm{ch}\,\pi\gamma - \sin q')}. \quad (4.11)$$

We have replaced summation over s by integration, and neglected terms of the type $q'/2\pi s$. Here $\zeta = (z/D) - n$, where n is the integer nearest to z/D. The main contribution to the integral with respect to q' is made by the integration in the vicinity of $q' = \pi/2$. Therefore when $\gamma \ll 1$ formula (4.11) can be rewritten in the form

$$T(z) = D\int_0^{\infty} ds 2\pi s \cos\left(2\pi s\zeta + \frac{\pi}{2}\frac{z}{D}\right) \int_{-\infty}^{\infty} \frac{d\alpha \exp\left(\frac{i\alpha z}{D}\right)}{(2\pi s)^3 - \frac{iM^3}{2}(\alpha^2 + \pi^2\gamma^2)}. \quad (4.12)$$

An analysis of this formula shows that when

$$M|\zeta| = \frac{|z - nD|}{\delta} \gg 1$$

the relative magnitude of the field between the peaks is small:

$$\left|\frac{T(z)}{T(nD)}\right| \leqslant \left|\frac{\delta}{z - nD}\right|^{1/2}. \quad (4.13)$$

The field distribution in the metal is shown schematically in Fig. 1. At $z \simeq nD$ there are sharp singularities (peaks), the width of which is of the order of several times δ.

The model considered by us, with a cylindrical Fermi surface, is not realized in any of the metals. In the best case the Fermi surface has individual sections that are nearly cylindrical (for example, in tin). This means that besides trajectories with nearly equal diameters there exist also trajectories with other values of D. If the diameter D depends significantly on p_H, then expression (4.3) must be averaged over p_H. In averaging the rapidly oscillating function $\sin(kD(p_H))$, the regions of values of p_H for which $D(p_H) = D_{ext}$ become singled out. The character of the singularities of $\sigma(k)$ is altered in this case, namely, the amplitude of the oscillating term in $\sigma(k)$ become small, on the order of $(kD_{ext})^{-1/2} \sim (\delta/D_{ext})^{1/2}$. For example, in the case of a Fermi sphere[10] with radius p_F we have

$$\sigma_{xx}(k) = \frac{3\sigma_0}{2kD_0}\left[1 - 2a\sin\left(kD_0 - \frac{\pi}{4}\right)\right], \quad (4.14)$$

$$a = \left(\frac{2}{\pi kD_0}\right)^{1/2} \simeq \left(\frac{2\delta}{\pi D_0}\right)^{1/2} \leqslant 1, \quad (4.15)$$

and $\sigma_0 = Ne^2/m\nu$ is the static conductivity of the metal and $D_0 = 2p_F c/eH$. Substituting (4.14) in (3.15) and expanding $T_{xx}(z)$ in powers of the small parameter a, we get

$$|T_{xx}(nD_0)| \approx a^n |T_{xx}(0)|. \quad (4.16)$$

The intensity of the peaks decreases exponentially with increasing number.

The difference between formulas (4.7)–(4.9) and (4.16) is of fundamental character. If all the electrons producing the skin layer are "focused" on a single plane, then a slowly damped system of bursts is produced. In the opposite case the damping is rapid: $T((n + 1)D)/T(nD) \sim a \ll 1$.

4.2. Chain of trajectories in an inclined magnetic field. A slowly damped system of peaks from chains of trajectories is possible not only in the case of a cylindrical Fermi surface. It should arise whenever the skin layer is determined, for some reason or another, not by all the effective trajectories, but only by a small fraction of them, for which the scatter ΔD of the diameters is small compared with the thickness of the skin layer δ:

$$\Delta D \ll \delta. \quad (4.17)$$

Let us ascertain the causes of the nonequivalence of the effective electrons. One of the possible mechanisms of such a selection was pointed out by Azbel' in[4]. In a metal with a complicated dispersion, the only electrons that take part in the cyclotron resonance are those having $\Omega(p_H) = \Omega_{ext}$. The extremum of $\Omega(p_H)$ is reached, in particular, on the central section $p_H = 0$ of the Fermi surface. The fraction of the resonant electrons is of the order of $(\nu/\Omega_{ext})^{1/2}$. On the other hand, the diameter of the electron trajectory $D(p_H)$ also has an extremum at $p_H = 0$. For resonant trajectories, the scatter of the diameters is $\Delta D \sim D_0(\Delta p_H/p)^2 \sim D_0\nu/\Omega$. If $\Delta D \ll \delta$, then the contribution made to the current by the all the nonresonant electrons can be neglected. Consequently, the high-frequency current is determined only by a small group of electrons near the section $p_H = 0$.

Another mechanism of selection of the effective electrons, proposed in[10], consists in the following. If we incline the vector H relative to the surface of the metal by a small angle φ, then the natural drift of the electrons along H, and consequently inside the metal, separates the electrons of the central section. These are precisely the electrons that have a small drift velocity and return many times to the skin layer. The remaining electrons can fall into the skin layer only once, after which they go either into the metal or collide with the surface of the sample. Therefore electrons with $p_H \approx 0$ play the dominant role in the creation of the skin current, and the mechanism of the "slowly damped chain of trajectories" is again in operation.

From the mathematical point of view, the mechanism of the AP of the field along a chain of trajectories is always due to the fact that the Fourier component of the conductivity $\sigma_{xx}(k)$ has minima at the points $k_n \sim 2\pi n/D$ that are located near the real axis of the complex variable k. This fact is illustrated by the cases (4.3) and (4.14) considered in the preceding section. In an inclined field, when the inequalities

$$\frac{(\delta D_0)^{1/2}}{l} \ll \varphi \leqslant \frac{\delta}{D_0} \quad (4.18)$$

are satisfied, the asymptotic expression for $\sigma_{xx}(k)$ has a similar form:

$$\sigma_{xx}(k) = \frac{3\sigma_0}{kl\varphi} \frac{1 - \sin kD_0 - w}{kD_0}, \quad (4.19)$$

where φ is the angle of inclination of the vector H rela-

tive to the surface of the metal. The parameter

$$w = \left(\frac{kD_0}{\pi}\right)^{1/2} \frac{1}{kl\varphi} \simeq \left(\frac{D_0\delta}{\pi l^2\varphi^2}\right)^{1/2} \qquad (4.20)$$

characterizes the scatter of the diameters of the electrons which return many times to the skin layer.

The inequalities (4.18) have a simple physical meaning. The relative number of electrons that have no time to go deeper into the metal during the mean free path time is $\delta/l\varphi$. The scatter of the diameters is $\Delta D \sim D_0(\Delta p_H/p_0)^2 \sim D_0\delta^2/l^2\varphi^2$. The condition (4.17) leads to the left-side inequality of (4.18). The right-side inequality of (4.18) states the requirement that just these electrons must make up the skin layer, i.e., that the small number of this group be compensated for by their repeated return to the skin layer: $(\delta/l\varphi)(l/D_0) \gg 1$. Thus, the natural drift of the electrons along the magnetic field plays the role of the selection mechanism that leads to weak damping of the peaks.

Since the Fourier component of the conductivity $\sigma_{xx}(k)$ has the same oscillating character as in the case of a cylindrical Fermi surface (see (4.3), the coefficient a of sin kD_0 is equal to unity, unlike in (4.14)), we present without a derivation the corresponding formulas for the function $T_{xx}(z)$ (for details see[10]):

$$T_{xx}(nD_0) = \delta \exp\left(\frac{\pi i}{8}\right) \cdot 2^{-3/2}\pi t_w(n), \qquad (4.21)$$

where

$$t_w(n) = \frac{1}{2\pi}\int_0^{2\pi} \frac{dq\cos nq}{(1 - w - \sin q)^{1/4}}, \qquad \delta = \left(\frac{e^2D_0 l\varphi}{12\pi\omega\sigma_0}\right)^{1/4}. \qquad (4.22)$$

When $n < (2w)^{-1/2}$ we have

$$t_w(n) = \frac{\cos\left(\frac{n\pi}{2}\right)}{(2\pi^2)^{1/4}} \frac{\Gamma\left(n + \frac{1}{4}\right)}{\Gamma\left(n + \frac{3}{4}\right)} \simeq \frac{\cos\left(\frac{n\pi}{2}\right)}{(2\pi^2)^{1/4} n^{1/2}},$$

$$t_w(0) = \Gamma^2\left(\frac{1}{4}\right)(2\pi^2)^{-3/4} \simeq 1.4. \qquad (4.23)$$

When $n > (2w)^{-1/2}$ the peaks are damped exponentially:

$$t_w(n) \simeq \frac{\Gamma\left(\frac{3}{4}\right)\cos\left(\frac{n\pi}{2}\right)}{\pi(16w)^{1/8} n^{3/4}} \exp\left(-n\sqrt{2w}\right). \qquad (4.24)$$

The damping of the peaks is due to the small yet finite scatter of the electron diameters relative to the central section. The distribution of the field in the metal in this case is illustrated in Fig. 1.

It must be emphasized that weak damping of the peaks in an inclined field is possible only if there is only one extremal diameter at a given orientation of the vector H. If the Fermi surface is non-convex or multiply connected, then the conductivity $\sigma_{xx}(k)$ is proportional to a sum of terms of the type of (4.19):

$$\sigma_{xx}(k) = \sum A_j(1 - \sin kD_j).$$

In the general case when the quantities A_j are of the same order, and the diameters D_j are not commensurate, $\sigma_{xx}(k)$ cannot vanish for any real value of k. Therefore the peaks of the field will attenuate exponentially just the same.

5. Anomalous Penetration due to Drift of Electrons Inside the Metal

5.1. Kinematics of open electron trajectories. Assume that on some periodic open trajectory with $\bar{v}_z \neq 0$

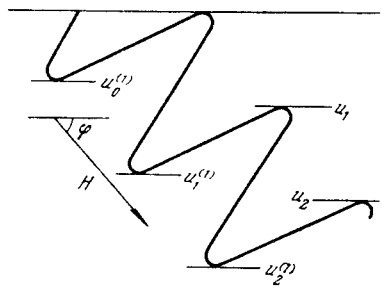

FIG. 3.

there is one effective point per period $2\pi/\Omega$. For the electron to interact with the alternating field it is necessary that one effective point of the trajectory be situated in the skin layer. Then the remaining points are situated at distances

$$u_n = nu \qquad (n = 1, 2, 3, \ldots), \qquad (5.1)$$

where u is the displacement of the electron along the z axis during the period $2\pi/\Omega$. If the trajectory has two effective points per period, then there appears, besides (5.1), one more sequence of depths

$$u_n^{(1)} = u^{(1)} + nu \qquad (u^{(1)} < u, \quad n = 0, 1, 2, \ldots), \qquad (5.2)$$

where $u^{(1)}$ is the projection of the distance between two neighboring effective points on the z axis (Fig. 3).

In accordance with the general concepts mentioned in the introduction, in order for a peak to occur it is necessary that the functions $u_n(p_H)$ and $u_n^{(1)}p_H$ have an extremum on the Fermi surface. It follows from (5.1) that all the u_n reach the extremum simultaneously. Consequently, one group of electrons is successively focused and produces peaks at the depths $z = nu_{ext}$. For the sequence $u_n^{(1)}$, this statement is generally speaking incorrect, since u and $u^{(1)}$ are two different functions of p_H. However, for sufficiently large n ($n > (u^{(1)'})^2/|u''|\delta$), both systems of peaks are produced practically by the same group of electrons with extremal values of $u(p_H)$. Therefore in most cases the singularities of the field AP due to the drift motion of the electrons are determined by the properties of the function $u(p_H)$. The presence of three and more effectiveness points in one period does not introduce anything new into this general picture.

Let us ascertain the conditions under which the electrons can drift deep into the metal. If the magnetic field is directed at an angle φ to the surface, then $\bar{v}_z$ differs from zero for all helical trajectories. The displacement u of the electron along the z axis within one period is determined by the formula

$$u = 2\pi\left|\frac{\bar{v}_z}{\Omega}\right| = \frac{2\pi mc}{eH}|\bar{v}_t| = \frac{c\sin\varphi}{eH}\left|\frac{\partial S(\varepsilon_F, p_H)}{\partial p_H}\right|. \qquad (5.3)$$

Let us consider in greater detail, by way of an example, the kinematics of the electrons in an inclined field on a spherical Fermi surface. We define the position of the orbit with the aid of the polar angle χ (Fig. 4). The values $\chi = 0$ and π correspond to the limiting points, and $\chi = \pi/2$ to the central section. On the orbits for which $\sin\chi > \sin\varphi$ there are two effective points each. The trajectories with $\chi = \varphi$ and $\pi - \varphi$ have one effective point per period each (see Fig. 2). The sections of the Fermi surface corresponding to $\sin\chi = \sin\varphi$ will be

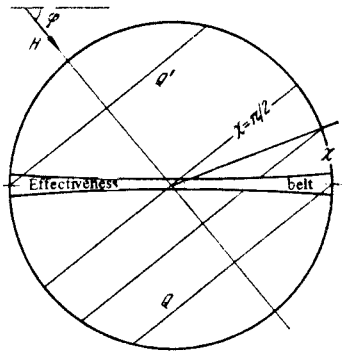

FIG. 4. Location of effective orbits on the Fermi sphere in an inclined magnetic field.

Q and Q' – boundary sections corresponding to the trajectory shown in Fig. 2.

called boundary sections. The remaining trajectories (with $\sin\chi < \sin\varphi$) are ineffective. The exact formula for $u(\chi)$ and $u_n^{(1)}(\chi)$ are of the form[5]

$$u(\chi) = \pi D_0 \sin\varphi\cos\chi, \qquad D_0 = 2p_F c/eH,$$

$$u_n^{(1)}(\chi) = D_0\sin\varphi\cos\chi\left[\pi n + \frac{(\mathrm{tg}^2\chi - \mathrm{tg}^2\varphi)^{1/2}}{\mathrm{tg}\,\varphi} - \arccos\left(\frac{\mathrm{tg}\,\varphi}{\mathrm{tg}\,\chi}\right)\right]. \quad (5.4)$$

Figure 5 shows the functions $u_1(\chi)$, $u_0^{(1)}(\chi)$, and $u_1^{(1)}(\chi)$ at different values of φ. It is seen from the figure that the curve $u_1^{(1)}(\chi)$ has two extrema at $\varphi \lesssim 25^\circ$. The $u_n^{(1)}$ with $n > 1$ behave in similar fashion.

At a small angle of inclination φ, the boundary sections $\tan\chi_{bound} = \cot\varphi$ are located near elliptic limiting points, where

$$\left|\frac{\partial S}{\partial p_H}\right| = 2\pi K_0^{-1/2}, \qquad u_0 = \frac{2\pi c\sin\varphi K_0^{-1/2}}{eH}, \quad (5.5)$$

and K_0 is the absolute value of the Gaussian curvature at the limiting point. On the Fermi sphere we have $K_0^{1/2} = p_F$. On a non-convex Fermi surface, extrema of $u(p_H)$ can occur also on other sections, where $\partial^2 S/\partial p_H^2 = 0$ and $\partial S/\partial p_H \neq 0$.

The focusing effect is possible also when $\varphi = 0$ in the presence of open Fermi surfaces. If the vector H lies in the plane of the sample and is orthogonal to the direction along which the Fermi surface is open, then the displacement u is the same on all open periodic trajectories and is determined by the formula

$$u = \frac{1}{eH} bc\cos\vartheta, \quad (5.6)$$

where b is the period of the open orbit and ϑ is the angle between the surface of the metal and the direction of the open part of the Fermi surface in p-space (see Sec. 2).

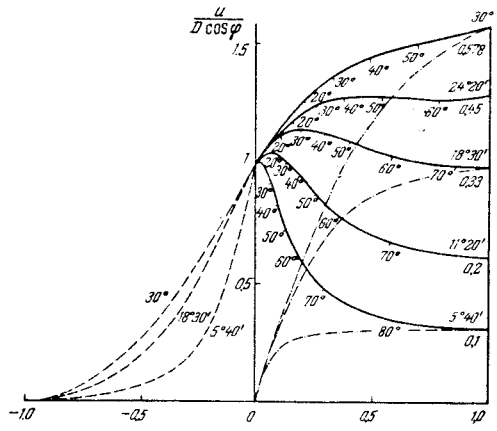

FIG. 5. Functions $u_1^{(1)}$ (solid lines, $u_0^{(1)}$ (dashed), and u_1 (dash-dot) for different inclination angles φ.

Abscissas – the quantity $\tan\varphi\cot\chi$. The values of the angle $\pi/2 - \chi$ are indicated along the $u_1^{(1)}$ curves. The angle φ and $\tan\varphi$ are indicated on the right.

5.2. Focusing of electrons from the vicinity of the limiting point at small angles of inclination of the magnetic field. As shown in[11], the field AP produced when the electrons drift into the metal can be analyzed by the method of Fourier transformation of the conductivity tensor, as described in Sec. 3. In the present section we describe another method of calculating the distribution of the field in the metal, which takes into account more consistently the collisions of the electrons with the surface of the metal[12].

Let us consider the field AP along the trajectories of the electrons from the vicinity of the limiting point. All are displaced equally along the vector H within the period $2\pi/\Omega$. This phenomenon is well known in electron optics as "focusing of monochromatic electrons by a longitudinal magnetic field." At large inclination angles φ there are no effective points on the orbits of the focusing electrons, since the limiting point is located far from the line $v_z = 0$. The electrons can be effective only in the case when the angle φ is sufficiently small. To this end it is necessary that the inclination angle φ, which is simultaneously the angular distance from the limiting points to the line $v_z = 0$, be smaller than the characteristic angular dimensions ψ of the region occupied on the Fermi surface by the focusing electrons. The value of ψ is determined from the condition that the spatial focusing of the electrons during the free-path time must not exceed δ, i.e.,

$$\frac{1}{v}|\bar{v}_z(\psi) - v_z(0)| \simeq \psi^2 l\sin\varphi \sim \delta, \quad \psi \sim \left(\frac{\delta}{l\sin\varphi}\right)^{1/2} \quad (5.7)$$

From this it follows that*

$$\sin\varphi < \left(\frac{\delta}{l}\right)^{1/3}. \quad (5.8)$$

On the other hand, the obvious condition $\delta \ll u_0$ leads to the inequality ($u_0 \sim D\sin\varphi$):

$$\frac{\delta}{D} \ll \sin\varphi. \quad (5.9)$$

In calculating the field distribution we shall start directly from formula (3.9) for the current density. This formula contains the function $s(z, \tau, \epsilon, p_H)$, which should be found from expression (3.8). The trajectories of the electrons from the vicinity of the limiting points are strongly elongated helices; in the zeroth approximation they can be replaced by straight lines. Then

$$s(z, \tau, \varepsilon, p_H) = \tau - \left(\frac{2\pi z}{u}\right) \qquad (\bar{v}_z > 0) \quad (5.10)$$

and $s = -\infty$ for negative $\bar{v}_z$. Inasmuch as for all the remaining electrons the form of the function s does not play any important role, we shall use expression (5.10) at all values of p_H in the calculation of the asymptotic

*A more accurate criterion on the side of larger φ is presented in the next section (formula (5.30)).

value of the y-component of the current density (3.9).

We use the saddle-point method in the integral over τ and τ' in (3.9). The saddle-points τ_α are the solutions of the equation $v_z(\tau_\alpha) = 0$, and coincide with the effective points. Using the saddle-point method in the integral with respect to τ, we get

$$j_\nu(z) = \frac{2e^2}{(2\pi\hbar)^3}\int \frac{m\,dp_H}{\Omega}\sum_{\tau_\alpha} v_\nu(\tau_\alpha)\int_{-\infty}^{\infty} dx \int_{s(z,\tau_\alpha p_H,\varepsilon_F)}^{\tau_\alpha} d\tau' v_\nu(\tau')$$
$$\times \exp\left[\frac{\nu - i\omega}{\Omega}(\tau'-\tau_\alpha)\right] E_\nu\left(z + \frac{1}{\Omega}\int_{\tau_\alpha}^{\tau'} d\tau'' v_x(\tau'') - \frac{v_z'(\tau_\alpha)}{2\Omega}x^2\right) \quad (5.11)$$

The summation is over all the τ_α in the interval from 0 to 2π. In the integral with respect to τ', one saddle-point coincides with the upper limit τ_α, and all the remaining ones are smaller than τ_α. Accordingly, we represent (5.11) in the form

$$j_\nu(z) = j_\nu^{(0)}(z) + \Delta j_\nu(z), \quad (5.12)$$

where $j_y^{(0)}(z)$ represents the contribution from the point $\tau' = \tau_\alpha$, and $\Delta j_y(z)$ represents the sum of all the remaining terms. After simple transformations we get

$$j_\nu^{(0)}(z) = A_\nu \int_{-\infty}^{\infty}\int d\xi\, d\eta E_\nu\left(z + \frac{1}{2}(\xi^2+\eta^2)\right), \quad (5.13)$$

where

$$A_\nu = \frac{e^2}{(2\pi\hbar)^3}\int dp_H \frac{m}{\Omega}\sum_{\tau_\alpha}\frac{v_\nu^2(\tau_\alpha)}{|v_z'(\tau_\alpha)|} \equiv \frac{e^2}{(2\pi\hbar)^3}\int d^3p v_\nu^2 \delta(v_z)\delta(\varepsilon-\varepsilon_F). \quad (5.14)$$

Going over to integration over the spherical image of the Fermi surface, we obtain

$$A_\nu = \frac{e^2}{(2\pi\hbar)^3}\oint \frac{d\lambda\cos^2\lambda}{K(\lambda)}, \quad (5.15)$$

λ is the azimuthal angle in velocity space ($v_z = v\cos\vartheta$, $v_y = v\sin\vartheta\cos\lambda$), ϑ is the polar angle, and the polar axis is parallel to Oz. For the Fermi sphere we have $A_y = 3Ne^2/8p_F$.

All the remaining saddle-points $\tau' = \tau_\alpha - 2\pi n$ make a contribution to $\Delta j_y(z)$. Out of the entire sum, we retain in $\Delta j_y(z)$ only one singular term, for which the value of nu is close to z. This is precisely the term responsible for the occurrence of the current peak

$$\Delta j_\nu(z) = \frac{2e^2}{(2\pi\hbar)^3}\oint \frac{d\lambda\cos^2\lambda}{K(\lambda)}\theta(z-nu)\exp\left(-2\pi n\frac{\nu-i\omega}{\Omega}\right)$$
$$\times\int_{-\infty}^{\infty}\int d\xi\, d\eta E_\nu\left[z - nu + \frac{1}{2}(\xi^2+\eta^2)\right], \quad (5.16)$$

where $\theta(x)$ is the unit step function: $\theta(x) = 1 (x > 0)$ and $\theta(x) = 0$ $(x < 0)$; $n = [z/u]$ is the integer part of z/u.

An important role in the integral with respect to λ is played by the small vicinity of the limiting point $\lambda = 0$, where $u(\lambda)$ has a maximum. Near this point, all the smooth functions of λ can be expanded in a series. As a result we obtain

$$\Delta j_\nu(z) = \frac{2e^2\exp\left[\frac{-z\left(1-\frac{i\omega}{\nu}\right)}{l_0\sin\varphi}\right]}{(2\pi\hbar)^3 K_0}\int_{-\infty}^{\infty}\int d\lambda\, d\xi\, d\eta\,\theta\left(z - nu_0 - \frac{1}{2}nu_0''\lambda^2\right)$$
$$\times E_\nu\left[z - nu_0 - \frac{1}{2}nu_0''\lambda^2 + \frac{1}{2}(\xi^2+\eta^2)\right], \quad (5.17)$$

where l_0 is the mean free path of the electron at the limiting point, and $u_0'' = \partial^2 u_0/\partial\lambda^2$. The characteristic width of the region of integration with respect to λ is of the order of $(\delta/z)^{1/2}$. This small parameter determines the relative magnitude of the current Δj_y in the peak compared with $j_y^{(0)}$. It is clear already from (5.17) that $\Delta j_y(z)$ is an almost periodic function of z with a period u_0, and attenuates exponentially over a length $l_0\sin\varphi$.

In view of the smallness of $\Delta j_y(z)$, Eq. (3.1) can be solved by perturbation theory. We use an even continuation of $E_y(z)$ for $j_y(z)$ and go over to the Fourier components (3.10). Equation (3.13) and the function $T_{yy}(z)$ are rewritten in the form

$$k^2\mathcal{E}_\nu(k) + 2E_\nu'(0) = 4\pi i\omega c^{-2}[\sigma_0(k)\mathcal{E}_\nu(k) + \Delta j_\nu(k)], \quad (5.18)$$
$$T_{yy}(z) = T_0(z) + \Delta T(z), \quad \sigma_0(k) = \frac{2\pi A_y}{|k|}, \quad (5.19)$$

where

$$T_0(z) = \int_0^\infty \frac{dk\cos kz}{k^2 - 4\pi i\omega c^{-2}\sigma_0(k)} \equiv \delta\int_0^\infty \frac{dqq\cos\left(\frac{qz}{\delta}\right)}{q^3 - i}, \quad (5.20)$$

$$\Delta T(z) = -\frac{2\pi i\omega}{c^2 E_y'(0)}\int_0^\infty \frac{dk\cos kz\,\Delta j_y(k)}{k^2 - 4\pi i\omega c^{-2}\sigma_0(k)}, \quad \delta = \left(\frac{c^2}{8\pi^2\omega A_y}\right)^{1/3}. \quad (5.21)$$

Figure 6 shows plots of the functions Re $2/\delta\, T_0(z)$ and Im $2/\delta\, T_0(z)$. These functions describe also the distribution of the field in the skin layer at H = 0 in the case of specular reflection of the electrons from the surface of the metal [11]. From (5.21) and (5.17) we get [12]

$$\Delta T(z) = -\left(\frac{8\delta^3}{\pi z}\right)^{1/2}\exp\left[-\frac{z\left(1-\frac{i\omega}{\nu}\right)}{l_0\sin\varphi}\right]\alpha\Psi_1\left(\frac{z-nu_0}{\delta}\right), \quad (5.22)$$

where

$$\alpha^{-1} = \left|\frac{u_0''}{u_0}\right|^{1/2}\frac{K_0}{\pi}\oint\frac{d\lambda\cos^2\lambda}{K(\lambda)}. \quad (5.23)$$

For a Fermi sphere $\alpha = 1$.

The function $\Psi_1(x)$ is of the form

$$\Psi_1(x) = \frac{1}{2i}\int_0^\infty \frac{dqq^{1/2}\cos\left(qx+\frac{\pi}{4}\right)}{(q^3-i)^2} + \frac{1}{2i}\int_0^\infty \frac{dqq^{3/2}\sin\left(qx+\frac{\pi}{4}\right)}{(q^3-i)(q^6+1)}[2\pi^{-1}q^2\ln q$$
$$+ 2\cdot 3^{-3/2}(q^4-1) + i\cdot 3^{-1}(2q^2+q+2)]. \quad (5.24)$$

Were we to disregard collisions between the electrons and the surface, and were we to use the distribution

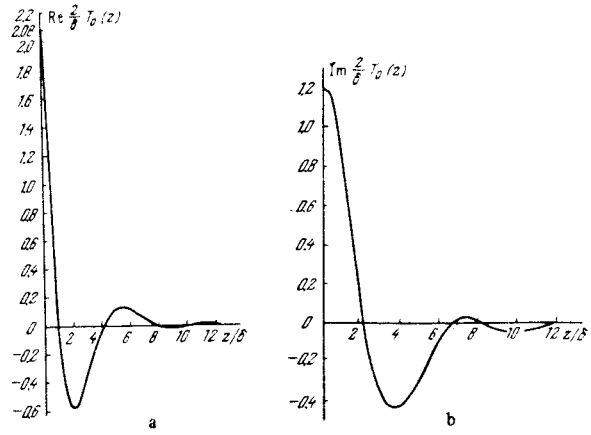

FIG. 6.

function in an unbounded metal, then there would be no θ-function in (5.16) and (5.17). Then (5.22) would contain in lieu of $\Psi_1(x)$ the function[11]

$$\Psi_2(x)=\frac{1}{i}\int_0^\infty \frac{dqq^{1/2}\cos\left(qx+\frac{\pi}{4}\right)}{(q^3-i)^2}. \qquad (5.25)$$

This expression would be obtained also if the field distribution were to be calculated by the Fourier expansion method (see Sec. 3). Figure 7 shows plots of Re $\Psi_{1,2}$ and Im $\Psi_{1,2}$ and of their derivatives. It is seen from these curves that allowance for collisions of the electrons with the surface of the metal leads to a decrease of the field on the left edge of the peak ($z < nu_0$) and hardly affects its shape when $z > nu_0$. (We shall return to a discussion of this fact in Sec. 11.) We see also that the real and imaginary parts of $\Psi_{1,2}$ (or $\Psi'_{1,2}$) change in such a manner that the extremum of one of them coincides with the position of the sharpest variation of the other. The characteristic spatial width of the burst is of the order of (6—7)δ and coincides approximately with the width of the function $T_0(z)$. The amplitude of the burst does not depend on H and decreases with increasing distance like $z^{-1/2}$.

The formulas presented in this section are valid in the case of focusing of electrons with an extremal displacement per period at large inclination angles φ of the vector $\vec{H}$ relative to the surface of the metal. The corresponding criterion for the applicability of the formulas is

$$kD\gamma \simeq \frac{D^2}{l\delta} \gg 1. \qquad (5.26)$$

Under ordinary experimental conditions this inequality is well satisfied. If it is replaced by the opposite inequality, then formula (5.22) describes directly the distribution of the field in the metal for the first peaks with numbers $n < u/\delta$.

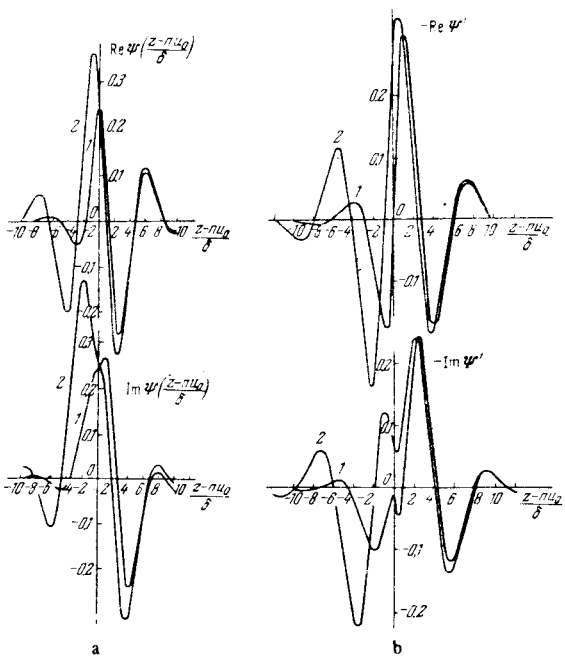

FIG. 7. Plots of the functions Ψ_1 and Ψ_2 (a) and of their derivatives Ψ'_1 and Ψ'_2 (b). The indices of the functions are indicated near the curves.

5.3. Focusing of electrons on the boundary section. "Quantization" of electron states in resonant interaction. When the angles of inclination of the magnetic field to the surface of the metal exceed $(\delta/l)^{1/3}$, the electrons are no longer effective in the vicinity of the limiting points. The projection of their velocity v_z does not vanish. Here, however, a different focusing mechanism of the effective electrons is possible[13]. The only effective electrons that resonate with the given harmonic of the wave packet are those for which the condition $ku = 2\pi n$ is satisfied. The current density in a metal with a given wave vector **k** is therefore determined only by the orbits corresponding to discrete values of the angle χ from the interval $\varphi < \chi < \pi - \varphi$ (see Fig. 4). The number of resonant states (i.e., the number of different groups of electrons) is determined by the wavelength $2\pi/k$, and by the magnitude and direction of the magnetic field. When any one of these parameters changes, the number of states also changes. In other words, a group of resonant particles can appear on the Fermi surface (or disappear). Because of this, the conductivity $\sigma(k)$ experiences finite increments (jumps). It is obvious that this effect is due to electrons situated in the vicinity of the boundary section of the Fermi surface, which separates the effective and ineffective electrons. The jumps of the conductivity $\sigma(k)$ lead to AP of the field in the metal as a result of the focusing of the electrons on the boundary section. Jumps of this kind, as is well known, are experienced by the density of the states and become manifest in all the macroscopic characteristics of the metals in a quantizing magnetic field when the number of Landau levels on the Fermi surface changes. In the case under consideration, the "quantization" of the states occurs under the classical conditions $\hbar\Omega \gg T$. This unique "quantization" of the states is due to the resonant interaction of the electrons with the variable field.

Let us investigate this AP mechanism, using as an example an alkali metal with a spherical Fermi surface. Since the velocity of the electron on the boundary section at the point $v_z = 0$ is directed along the y axis, it is necessary to calculate the conductivity $\sigma_{yy}(k)$ and the corresponding field distribution function $T_{yy}(z)$.

In this and following sections we shall disregard the collisions between the electrons and the metal surface, and we shall use the Fourier-transformation method described in Sec. 3. In addition, we confine ourselves to the low-frequency case (3.19). From the general formula (3.12) we get

$$\sigma_{yy}(k)\equiv\sigma(k)=\frac{3Ne^2}{4\pi m\Omega}\int_{-1}^{1}d\mu\int_0^{2\pi}d\tau\, n_y(\tau,\mu)\int_{-\infty}^{\tau}d\tau' n_y(\tau',\mu)\exp[\gamma(\tau'-\tau)]$$
$$\times\cos[kR\mu\sin\varphi(\tau'-\tau)+kR\cos\varphi(1-\mu^2)^{1/2}(\cos\tau'-\cos\tau)]. \qquad (5.27)$$

We have introduced here the following notation: $\mu = \cos\chi$, χ—angle between **v** and **H**, and

$$n_y\equiv v_y/v=\mu\cos\varphi+(1-\mu^2)^{1/2}\sin\varphi\sin\tau,\quad \gamma=\nu/\Omega.$$

Expanding the cosine in (5.27) in a double Fourier series in τ and τ', and calculating the integrals, we get

$$\sigma(k)=\frac{3Ne^2}{2m\Omega\cos^2\varphi}\sum_{n=-\infty}^{\infty}{}'\int_{-1}^{1}\frac{d\mu\gamma J_n^2(kR\cos\varphi\sqrt{1-\mu^2})}{\gamma^2+(n-kR\mu\sin\varphi)^2}(\mu\cos^2\varphi+n\sin\varphi(kR)^{-1})^2. \qquad (5.28)$$

If we let the mean free path l go to infinity, then $\gamma \to 0$, and

$$D(x) = \frac{\gamma}{\pi(\gamma^2 + x^2)} \to \delta(x). \quad (5.29)$$

In order to obtain the condition for the validity of such a substitution at finite values of γ, it is necessary to compare the relative rate of change of the two rapidly varying functions $D(n - kR\mu\sin\varphi)$ and $J_n(kR\cos\varphi\sqrt{1-\mu^2})$. It will be seen from the exposition that follows that an important role in the sum over n is played by the terms with

$$|n| \equiv n_0 = \left[\frac{kR}{2}\sin 2\varphi\right].$$

When $|n| = n_0$, the D-function has a maximum at $|\mu| = \cos\varphi$, the width of the maximum being $\Delta\mu \sim \gamma/kR\sin\varphi$. The Bessel function $J_n(kR\cos\varphi\sqrt{1-\mu^2})$ changes near the maximum of the D-function over the interval $\Delta\mu \sim (\sin^2\varphi/kR)^{2/3}$. This estimate follows from the well-known asymptotic expression for the Bessel function $J_n(x)$ when $n \sim x \gg 1$. Therefore the condition for the replacement of the D-function by a δ-function in (5.28) is

$$\frac{\gamma}{kR\sin\varphi} \ll \left(\frac{\sin^2\varphi}{kR}\right)^{2/3} \quad \text{or} \quad \sin\varphi > \left(\frac{R^2}{kl^3}\right)^{1/7}. \quad (5.30)$$

The quantity $\varphi_c \sim (R^2\delta/l^3)^{1/7}$ (and not $(\delta/l)^{1/3}$) plays the role of the critical inclination angle: when $\varphi < \varphi_c$ the electrons of the limiting point can still be regarded as effective, but in the region $\varphi > \varphi_c$ they are ineffective. When condition (5.30) is satisfied, formula (5.28) can be represented in the form

$$\sigma(k) = \frac{3\pi\sigma_0}{2kl\sin\varphi}\sum\left(\frac{n}{kR\sin\varphi\cos\varphi}\right)^2 J_n^2[(k^2R^2\cos^2\varphi - n^2\operatorname{tg}^2\varphi)^{1/2}]. \quad (5.31)$$

The summation is over all the n (positive and negative) for which the radical in the argument of the Bessel function is real.

Expression (5.31), in which the integral over the states is replaced by the sum over the discrete values of n, illustrates the statement made above concerning the "quantization" of the electron states as a result of the resonant interaction of the electrons with the electromagnetic field. Formula (5.31) is asymptotically exact when $\gamma \to 0$ and takes into account the contribution of both the effective and ineffective electrons. The difference between their interactions with the wave is connected with the change of the character of the asymptotic form of the Bessel function $J_n(x)$ when $n \sim x \gg 1$ (the Stokes phenomenon[14]). For the effective electrons ($x > n \gg 1$), the asymptotic form of $J_n(x)$ is oscillating and for the ineffective particles ($n > x$) the function $J_n(x)$ decreases exponentially. The "turning point" $x = n$ corresponds in our case to the boundary section, and with this $|n| = n_0$. The condition under which all the ineffective electrons with $|n| > n_0$ make an exponentially small contribution is determined by the inequality $n^2 - x^2 \gg n_0^{4/3}$. In particular, it should be satisfied also for $|n| = n_0 + 1$. From this we get the criterion for φ on the side of large angles

$$\sin^2\varphi \gg n_0^{-1/3} \quad \text{or} \quad \sin\varphi < (kR\cos\varphi)^{-1/7}. \quad (5.32)$$

It follows from (5.30) and (5.32) that the angle region in which the electrons should become focused on the boundary section is bounded by the inequalities

$$\gamma^{3/7}(kR)^{-1/7} \ll \sin\varphi < (kR)^{-1/7}. \quad (5.33)$$

In the sum over n it is possible to disregard here the exponentially small terms with $|n| > n_0$.

For large values of kR sin φ, many values of n are important in the sum over n. Using the asymptotic form of the Bessel functions and replacing the sum over n by an integral, we get

$$\sigma^{(0)}(k) = \frac{3\sigma_0}{2kln_0^2}\int_{-n_0}^{n_0}\frac{dnn^2}{(n_0^2-n^2)^{1/2}} = \frac{3\pi\sigma_0}{4kl}. \quad (5.34)$$

The "quantum effect," which is manifest in the difference between the sum over n and the integral, is due to terms with $|n| = n_0$. When the inequality (5.32) is satisfied, these terms decrease exponentially in a region where the argument of the corresponding Bessel function is smaller than the index. Therefore

$$\frac{\Delta\sigma(k)}{\sigma^{(0)}(k)} = \frac{4}{\sin\varphi}J_{n_0}^2(n_0)\,\theta(kR\sin\varphi\cos\varphi - n_0) \simeq \frac{a_0}{\sin\varphi(ku)^{2/3}}\theta\left(\frac{ku}{2\pi} - n_0\right),$$

$$a_0 = \frac{(12\pi)^{2/3}\Gamma^2\left(\frac{1}{3}\right)}{3\pi^2} \simeq 2.75, \quad (5.35)$$

where $u = 2\pi R\sin\varphi\cos\varphi$ is the displacement of the electron on the boundary section along the z axis. The region of "smearing" of the θ-function is of the order of $(2\pi ku)^{1/3}\sin^2\varphi$ and is small as a result of the inequality (5.32). The dependence of $\Delta\sigma(k)$ on

$$\Delta = \frac{ku}{2\pi} - \left[\frac{ku}{2\pi}\right]$$

when $\Delta < 0$ is described by the function

$$\exp\left[-\frac{1}{3}\left(\frac{2|\Delta|}{n_0^{1/3}\sin^2\varphi}\right)^{3/2}\right]. \quad (5.36)$$

Thus, the Fourier component of the conductivity $\sigma(k)$ experiences jumps when k is varied in the angle region (5.33).

The distribution of the electromagnetic field in the metal is described by the function (3.15). Integrating this expression by parts and omitting certain indices, we obtain

$$T(z) = \frac{1}{z}\int_0^\infty \frac{dk\sin kz}{[k^2 - 4\pi i\omega c^{-2}\sigma(k)]}\frac{d}{dk}[k^2 - 4\pi i\omega c^{-2}\sigma(k)]. \quad (5.37)$$

In the differentiation of the smooth functions k, we obtain the function $T_0(z)$ (5.20), which decreases sharply near the surface and has no singularities in the volume of the metal. The field peaks are due to the derivative of the θ function in (5.35) and are described by the formula

$$\Delta T(z) \equiv T(z) - T_0(z) = -\frac{ia_0u^2M^3}{z\sin\varphi}\sum_{s=0}^{\infty}{}'\frac{(2\pi s)^{1/3}\sin(2\pi sz\,u)}{[(2\pi s)^3 - iM^3]^2},$$

$$M = \frac{u}{\delta}, \quad \delta = \left(\frac{c^2l}{3\pi^2\omega\sigma_0}\right)^{1/3}. \quad (5.38)$$

The sum (5.38) represents a periodic function of z with a period u. At large values of M it has singularities whose form is determined by the expression

$$\Delta T(z) = \frac{a_0\delta(u\delta^2)^{1/3}}{2\pi z\sin\varphi}\Psi_3\left(\frac{z-nu}{\delta}\right), \quad \Psi_3(x) = \frac{1}{i}\int_0^\infty \frac{dqq^{1/3}\sin qx}{(q^3-i)^2}. \quad (5.39)$$

In the derivation of these formulas we disregarded the "smearing" of the θ-function (5.36), which leads to an

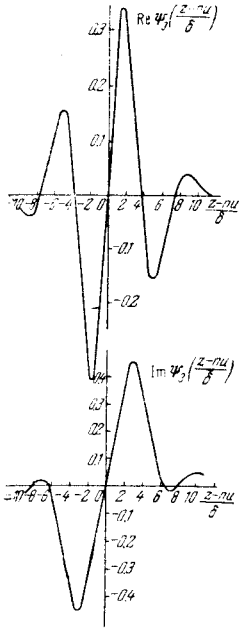

FIG. 8

exponential decrease of the peaks over distances $L \sim (u^2\delta)^{1/3}/\sin^2\varphi$. Because of inequality (5.32), we get $L \gg u$. The amplitudes of the first few singularities decrease with depth like z^{-1}. Figure 8 shows the field distribution near the singularity.

5.4. Focusing of effective electrons on open periodic trajectories. Let us consider the AP of the field in a metal with an open Fermi surface in the case when the vector **H** is parallel to the boundary of the sample. If we disregard the collisions of the electrons with the surface of the metal, then it is convenient to use in the calculation of the field distribution the Fourier expansion method (Sec. 3). Calculating the integrals with respect to τ and τ' in (3.12) for the elements of the conductivity tensor $\sigma_{\alpha\beta}(k)$ with the aid of the stationary-phase method, we obtain[11]

$$\sigma_{\alpha\beta}(k) = \frac{2e^2}{(2\pi\hbar)^3|k|}\left\{\int\limits_{\text{closed}}\frac{d\lambda n_\alpha n_\beta}{K\gamma} + \int\limits_{\text{open}}\frac{d\lambda n_\alpha n_\beta}{K}\frac{\gamma}{\gamma^2+\pi^{-2}\sin^2\left(\frac{ku}{2}\right)}\right\}. \tag{5.40}$$

The integration is along the line $v_z = 0$ ($\vartheta = \pi/2$) on the Fermi surface, $n_\alpha = v_\alpha/v$ are the components of the unit velocity vector, and ϑ and λ are the polar and azimuthal angles in velocity space. The first term represents the contribution of the closed orbits, where the displacement $u \equiv 0$, and the second is due to the open orbits in p-space, on which u is constant and is given by (5.6). Inasmuch as γ changes smoothly within the open-orbit layer, the resonant factor can be taken outside the integral with respect to λ, replacing γ by certain characteristic value γ_0.

In (5.40) we neglected the contribution of the stationary-phase points that lead to a sequence of peaks at depths $z = u_n^{(1)}$ (see Sec. 5.1). Following[11], we assume that the relative "number" of open orbits is small, i.e., the second term in (5.40) is a small correction. The basis for such an assumption is the fact that the role of the open orbits is significant only in a small interval of values of ku, where $|ku - 2\pi n| \lesssim \gamma$. At all other values of ku, the second term of (5.40) is of relative order of smallness $\gamma_0^2 \ll 1$. Since the field distribution in the metal is determined by the integral with respect to k, the singularity in the field distribution has a relative amplitude of the order of γ_0.

We refer the first term in (5.40) to the principal axes. In terms of these axes

$$\sigma_{\mu\mu}^{(k)} = \frac{3\pi}{4|k|}B_{\mu\mu}\left(1+\beta_{\mu\mu}\frac{\gamma_0^2}{\gamma_0^2+\pi^{-2}\sin^2\left(\frac{ku}{2}\right)}\right),$$

$$B_{\mu\mu} = \frac{e^2}{3\pi^4\hbar^3}\int\limits_{\text{closed}}\frac{d\lambda n_u^2}{K\gamma}, \tag{5.41}$$

where $\beta_{\mu\mu}$ is the relative "number" of open orbits. We shall henceforth omit the vector indices. Let us investigate the field distribution function in the metal (3.15). The field near the surface is described by formula (5.20), in which the depth δ of the skin layer is of the form

$$\delta \sim \left(\frac{c^2}{3\pi^2\omega B}\right)^{1/3}. \tag{5.42}$$

The form of the peaks and their decrease with depth are determined by the function

$$\Delta T(z) = iM^3\beta\gamma_0 u\int\limits_0^\infty \frac{dx\, x\cos\left(\frac{xz}{u}\right)}{(x^3-iM^3)^2}\frac{\gamma_0}{\gamma_0^2+\pi^{-2}\sin^2\frac{x}{2}}, \tag{5.43}$$

where $M = u/\delta \gg 1$. The main contribution to the integral in (5.43) is made by integration near the points $x \equiv ku = 2\pi s$ (s—integer). Therefore

$$\Delta T(z) = 2\pi^2 iM^3\beta\gamma_0 u\sum_{s=0}^{\infty}\frac{2\pi s\cos\left(\frac{2\pi sz}{u}\right)}{|(2\pi s)^3-iM^3|^2}\exp\left(-\frac{2\pi\gamma_0 z}{u}\right). \tag{5.44}$$

The function $\Delta T(z)$ is an almost periodic function of z with a period u. At large values of z, the field in the metal is an aggregate of narrow and slowly-decreasing peaks. The form of the singularity near $z = nu$ is

$$\Delta T(z) = -\pi\beta\gamma_0\delta\exp(-2\pi n\gamma_0)\,\Psi_4\left(\frac{z-nu}{\delta}\right), \qquad \Psi_4(x) = \frac{1}{i}\int\limits_0^\infty\frac{dq\,q\cos qx}{(q^3-i)^2}. \tag{5.45}$$

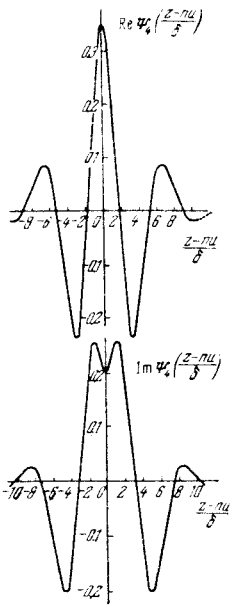

FIG. 9

Plots of Re $\Psi_4(x)$ and Im $\Psi_4(x)$ are shown in Fig. 9. Just as in the case of the limiting point, the extremum of one of the curves coincides approximately with the position of the sharpest variation of the other. The width of the peak is $(5-7)\delta$, the relative height of the peak is of the order of $\beta\gamma_0$ and is small compared with the field on the surface even when $\beta \sim 1$. The exponential decrease of the bursts occurs over a characteristic length l of the mean free path of the electrons on the open orbits. From the mathematical point of view, the AP of the field into a metal as a result of focusing of effective electrons on open periodic orbits is connected with the delta-like singularities of the Fourier components of the conductivity tensor (5.40).

6. Focusing of Ineffective Electrons

The ineffective electrons move over trajectories such that their velocity component v_z normal to the surface of the metal never vanishes. The interaction with the electromagnetic field is resonant only for that wave-packet harmonic, whose length is equal to the displacement of the electron u within one period. Because of this, a field AP having a harmonic character is produced in the metal[15]. The spatial period of the oscillations is determined by the extremal values of the displacement u_{ext} (Sec. 5.1). From the mathematical point of view the difference between the ineffective electrons and the effective ones is manifest in the fact that the Fourier component of the conductivity $\sigma(k)$ has a single singular point, located near the real axis on the complex k-plane.

The considered mechanism of AP of the electromagnetic field has an analogy in static conductivity. Sondheimer[16] and later V. L. Gurevich[17] have shown that the resistance of metal plates in a normal magnetic field oscillates with variation of H. The oscillations are connected with the change of the number of revolutions of the electron on the path from one surface of the plate to the other. This phenomenon was first observed by Babiskin and Siebenmann[18] and by a number of other workers[19,20].

Let us consider the simplest case, when the vector H is perpendicular to the boundary of the metal, and the Fermi surface is singly-connected and is actually symmetrical with respect to the z axis. It is known[21] that in this case it is convenient to introduce circularly polarized quantities

$$E_\pm(z) = E_x(z) \pm iE_y(z) = -2\pi^{-1}E'_\pm(0)\,T_\pm(z), \tag{6.1}$$

$$T_\pm(z) = \frac{1}{2}\int_0^\infty \frac{dk\,[\exp(ikz) - \exp(-ikz)]}{k^2 - 4\pi i\omega c^{-2}\sigma_\pm(k)}. \tag{6.2}$$

The Fourier components of the conductivity $\sigma_\pm(k)$ are given by

$$\sigma_\pm(k) = \frac{2\pi e^2}{(2\pi\hbar)^3}\int dp_z \frac{mv_\perp^2}{\Omega}[\gamma + iY_\mp(p_z)]^{-1}, \quad Y_\pm(p_z) = \frac{ku(p_z)}{2\pi} \pm 1, \tag{6.3}$$

where $v_\perp = (v_x^2 + v_y^2)^{1/2}$ is the transverse velocity. The symbols $\pm$ in (6.3) correspond to electrons, and should be interchanged in the case of holes. Formula (6.3) can be easily obtained from (3.12) if it is assumed that projection of the velocity v_z does not depend on τ and if we put $v_x = v_\perp \cos\tau$ and $v_y = v_\perp \sin\tau$.

It is known from[1] that in the anomalous skin effect the electromagnetic field at large distances from the surface of the metal consists of two components. One represents the contribution from the poles of the integrand of (6.2) and describes the sharp decrease of the field near the surface of the metal. This part of the field is due to the effective electrons. The second is connected with the presence of a single branch point in the Fourier component of the conductivity $\sigma_\pm(k)$. The singular points of $\sigma_\pm(k)$ are due to the contribution of the electrons from the vicinity of the limiting point of the Fermi surface, or else from the section where $u(p_z) = u_{ext}$. In a strong magnetic field these points are located near the real k axis. At large distances from the surface of the metal, the contribution of the effective electrons (poles) can be neglected, and the behavior of the field is determined by the form of the functions $\sigma_\pm(k)$ in the vicinity of the singular points.

6.1. Limiting point. The contribution to the connectivity from the electrons of the limiting point is determined by the expression

$$\begin{aligned}\Delta\sigma_\pm(k) &= \frac{2\pi e^2 m}{(2\pi\hbar)^3\Omega}\frac{dv_\perp^2}{dp_z}\left\{\int_{-p_0}^{p_0}\frac{dp_z\,(p_z - p_0)}{\gamma - iY_\mp(p_0) + iY'_\mp(p_0)(p_z - p_0)} - \int_{-p_0}^{p_0}\frac{dp_z\,(p_z + p_0)}{\gamma - iY_\pm(p_0) + iY'_\pm(p_0)(p_z - p_0)}\right\}\\ &= -\frac{ie^2 m}{\hbar^3\Omega(ku'_0)^2}\frac{dv_\perp^2}{dp_z}[(Y_\mp(p_0) - i\gamma)\ln(Y_\mp(p_0) - i\gamma) + (-i\gamma - Y_\pm(p_0))\ln(-i\gamma - Y_\pm(p_0))].\end{aligned} \tag{6.4}$$

The integration is near the limiting points $p_z = \pm p_0$, $Y'_\pm = \partial Y_\pm/\partial p_z$. It follows from (6.4) that near Re $k > 0$ the function $\Delta\sigma_+(k)$ has a singularity of the type $x \ln x$ at $k_+u_0 = 2\pi(1 + i\gamma)$, and the function $\Delta\sigma_-(k)$ has a singularity at $k_-u_0 = 2\pi(1 - i\gamma)$. Let us calculate, for example, the asymptotic expression for $T_+(z)$ at large values of z. We make a cut in the complex k plane from k_+ to $k_+ + i\infty$. In the term with exp(ikz) of formula (6.2) we turn the contour to Im $k > 0$, and in the term with exp(−ikz) we make the turn to Im $k < 0$. The integral (6.2) can be represented in the form of a sum of residues and an integral along the edges of the cut, since the sum of the integrals along the imaginary axis vanishes identically. The sum of residues, as indicated above, decreases rapidly, since the roots of the equation $k^2c^2 = 4\pi i\omega\sigma_+(k)$ are complex: $k_j = \delta^{-1}\epsilon_j$, $\epsilon_j^3 = i$. The quantity δ is the depth of penetration of the field into the metal at $H = 0$ and is determined by the formula (5.21). Therefore in the asymptotic expression $T_+(z)$ there remains only the integral along the edges of the cut. The calculations carried out in[15] lead to the following result:

$$T_+(z) = A_0 z^{-2}\exp\left(ik_+z - \frac{\pi i}{2}\right), \tag{6.5}$$

where

$$A_0 = \frac{e^2c^2}{(4\pi)^2\hbar^3}\left(\frac{mv_z}{\Omega}\frac{\partial v^2}{\partial p_z}\right)_{p_0}\left(\frac{u_0}{u_0'}\right)^2\sigma_+^{-2}\left(\frac{2\pi}{u_0'}\right). \tag{6.6}$$

For a spherical Fermi surface we get

$$A_0 = \frac{\pi^2}{8}\delta^3, \quad \delta = \left(\frac{cp_F}{3\pi^2\omega Ne^2}\right)^{1/3}. \tag{6.7}$$

In the presence of several limiting points, the oscillations can have different phases, owing to the complex nature of the quantities $\sigma_+(2\pi/u_0')$. From (6.5) it

follows that in the case of linear polarization the field in the metal is a standing wave ($\sim \cos(2\pi z/u_0)$).

6.2. Helical trajectories with extremal displacement over the period. In the vicinity of the corresponding branch point $\sigma_\pm(k)$ is given by

$$\sigma_\pm(k) = \frac{2\pi e^2 m v_\perp^2}{(2\pi\hbar)^3\Omega}\int_{-\infty}^{\infty} dp_z \left\{\left[\gamma + iY_\mp(p_1) - \frac{i}{2}|Y_\mp'(p_1)|(p_z-p_1)^2\right]^{-1} + \left[\gamma - iY_\pm(p_1) + \frac{i}{2}|Y_\pm''(p_1)|(p_z-p_1)^2\right]^{-1}\right\} \simeq \frac{e^2 m v_\perp^2}{\hbar^3\pi\Omega}\left|\frac{2u_1}{u_1''}\right|^{1/2}\frac{(\pm i)}{(\pm\gamma i - Y_-(p_1))^{1/2}} \qquad (6.8)$$

The values of all the quantities are taken at $|p_z| = p_y$, where the function $u(p_z)$ has an extremum, $u'' = \partial^2 u(p_1)/\partial p_z^2$. Unlike the case of the limiting point, in (6.8) there appears a singularity of the type $x^{-1/2}$ at $k_\pm \simeq 2\pi/u_1$. Calculations similar to those given above yield the following field distribution:

$$T_\pm(z) = A_1(u_1 z^3)^{-1/2}\exp\left(ik_\pm z \pm \frac{\pi i}{4}\right), \qquad (6.9)$$

$$A_1 = \frac{\pi k^3 c^2 |v_z|}{2\omega^2 m v_\perp^2}\left|\frac{u_1''}{u_1}\right|^{1/2} \sim \delta^3. \qquad (6.10)$$

All the formulas presented above are valid when the conditions $\delta \ll u \ll l, z$ are satisfied. From a comparison of (6.9) and (6.5) it is seen that the amplitude of the oscillations is larger by a factor $(z/u)^{1/2}$ in the case of extremal helical trajectories than in the case of a limiting point. The amplitude of the oscillations due to the electrons near the limiting point is independent of H in this case.

6.3. Open orbits. Drift of the ineffective electrons into the metal is possible also when the magnetic field is parallel to the surface[22]. To this end it is necessary that the Fermi surface be open and the vector H be orthogonal to the mean direction of the opening. It can be shown if the electrons on the open periodic orbits are ineffective, and the corresponding tangential component of the velocity contains only the first harmonic in τ, then the following formula is valid for $\sigma(k)$

$$\sigma(k) = \frac{3\pi B}{4|k|}\left\{1 + \beta\gamma_0^2\left[\gamma_0^2 + \left(1 - \frac{ku}{2\pi}\right)^2\right]^{-1}\right\}. \qquad (6.11)$$

Expression (6.11) is obtained from (5.41) if account is taken in the latter of the resonant interaction with only one component of the wave packet. The field AP is described in this case by the function

$$\Delta T(z) = i\omega^4\beta\gamma_0\delta^{-3}\int_0^\infty \frac{dx\exp\left(\frac{xz}{u}\right)}{\left[x^3 - i\left(\frac{u}{\delta_0}\right)^3\right]^2\gamma_0^2 + \left(1 - \frac{x}{2\pi}\right)^2} \simeq A_2\cos\left(\frac{2\pi z}{u}\right)\exp\left(-\frac{z}{l}\right), \quad A_2 = \frac{\pi\beta\delta_0^3}{iul}, \qquad (6.12)$$

where δ is determined by (5.42).

The amplitude of the harmonic oscillations (6.12) decreases slowly over the characteristic length l of the mean free path of the electrons on the open trajectories. The quantity A_2 does not depend on the magnetic field and is of the order of $\beta\delta_0^3 l$, where δ_0 is the depth of the skin layer at H = 0.

We have considered above only the simplest cases, when the normal component of the velocity v_z does not depend on τ, and the tangential components of the velocity contain only the first harmonics in τ. In the general case when v_z depends on τ and higher components are present in the Fourier expansions of $v_x(\tau)$ and $v_y(\tau)$, higher harmonics of the type $\cos(2\pi nz/u)$ appear also in the distribution of the field E(z). When v_z is strongly dependent on τ, effective points $v_z(\tau) = 0$ can occur on the trajectories of the drifting electrons. In this case the AP can be interpreted as propagation in the metal of a large number of weakly-damped harmonic plane waves, the interference of which causes the appearance of the narrow peaks. The dependence of v_z on τ should also lead to a dependence of the amplitude of the harmonic oscillations on the polarization of the external field. For an elliptic limiting point the degree of ellipticity of the standing wave coincides with the ellipticity of the limiting point.

7. Singularities of Anomalous Penetration of the Field Into a Metal at High Frequencies. New Mechanisms of Cyclotron Resonance

So far we have considered the AP of a field into a metal at low frequencies (3.19). Obviously, the AP mechanisms described above are effective also at high frequencies $\omega \gg \nu$. A characteristic property of metals in this region of frequencies is the resonant dependence of the surface impedance on the magnetic field. The cyclotron resonance (CR) connected with multiple return of the effective electrons to the skin layer is most sharply manifest when the vector H is parallel to the surface of the metal. At large inclination angles $\varphi \gg \delta/l$, most electrons fall into the skin layer only once, after which they go off into the metal or else collide with its surface. In this case the CR due to multiple return of the effective electrons to the skin layer becomes impossible. The existence and the singularities of CR in an inclined magnetic field[23] are connected with the AP of electromagnetic waves in the metal.

7.1. Chain of trajectories in an inclined magnetic field and cyclotron resonance. Let us consider a metal with a spherical Fermi surface. Under the conditions of strict resonance $\omega = n\Omega$, the field distribution in the metal will be practically the same as at low frequencies (see Sec. 4.2). With increasing "detuning" of the resonance, an increase takes place in the "dephasing" of the electrons that produce the peaks, and the amplitude of the peaks decreases[10]. Accordingly, the impedance increment Δz_{res} due to the field AP in the metal along the trajectory chain should experience resonance oscillations. In a parallel field, this addition is a small correction to the main effect. In an inclined field, it plays a decisive role in determining the form and the amplitude of the CR.

According to[23], the Fourier component of the conductivity $\sigma_{xx}(k)$ is of the form (we omit the vector indices)

$$\sigma(k) = \frac{3Ne^2}{2m}\sum_{n=-\infty}^{\infty}\int_{-1}^{1}\frac{d\mu\,(1-\mu^2)\,[J_n'(kR\cos\varphi\sqrt{1-\mu^2})]^2}{\nu - i(\omega - n\Omega - kv\mu\sin\varphi)}. \qquad (7.1)$$

This formula can be obtained directly from the general expression (3.12), by calculating the integrals with respect to τ and τ'. The effect considered by us takes place in the region of small inclination angles $\varphi < (\delta/D)^{1/2} \ll 1$. Therefore all the functions φ in (7.1)

can be expanded in series, retaining the first nonvanishing terms of the expansion. The region of small φ breaks up in turn into several regions, depending on the efficiency of the mechanism by which the electrons are selected by diameters as a result of their drift motion.

In the angle interval

$$\frac{\delta}{l} < \varphi < \frac{(\delta D_0)^{1/2}}{l} \tag{7.2}$$

the scatter of the diameters of electrons with small $|\mu|$ is much larger than the depth δ (see Sec. 4.2). Therefore the field peaks attenuate rapidly with increasing distance, and the amplitude of Δz_{res} is small. The conductivity $\sigma(k)$ has in this region the form

$$\sigma(k) = \frac{3\sigma_0}{klkD_0\varphi}\left[1 - \frac{\sqrt{2}}{\pi w}\sin(kD_0 - n\pi)\right]. \tag{7.3}$$

The parameter

$$w = \left(\frac{kD_0}{\pi}\right)^{1/2}\frac{\nu - i\Delta\omega}{kv\varphi} \qquad (\Delta\omega = \omega - n\Omega) \tag{7.4}$$

characterizes the scatter of the diameters of the electrons that return many times to the skin layer (cf. (4.20)) and in the region (7.2) we have $|w| \gg 1$.

Owing to the smallness of the oscillating term in (7.3), the field peaks decrease exponentially (see (4.14) and (4.16)):

$$T(nD_0) \sim (\pi w)^{-n} T(0), \tag{7.5}$$

and their amplitude has a resonant dependence on the magnetic field. The resonant addition to the impedance of the half-space is due to the first peak, which is located at the depth $z = D_0$. As they move along the trajectory, the electrons return to the surface of the metal $z = 0$ a part of the field ($\sim w^{-1}$) of the first peak, which is weaker by a factor w^{-1} than the field on the surface itself. Indeed, if we substitute (7.3) in (3.18) and expand T(0) in powers of the small parameter 1/w, we get

$$\Delta Z_{res} = Z - Z_0 = \frac{\omega(l\varphi)^2}{\pi c^2 D_0}\frac{2\Lambda - i(1-\Delta^2)}{1-\Delta^2}, \qquad \Delta = \frac{\Delta\omega}{\nu}, \tag{7.6}$$

$$Z_0 = 2^{3/2}\pi\omega\delta c^{-2}\exp\left(-\frac{3\pi i}{8}\right), \tag{7.7}$$

where δ is given by (4.22). The relative amplitude of the resonance, obviously, is of the order of $(l\varphi/\sqrt{2\pi D_0\delta})^2$. Figure 10 shows the dependence of the real and imaginary parts of the resonant addition to the impedance on Ω^{-1}.

In the region (4.18), the selection of electrons by diameters is quite effective, and the field peaks along the trajectory chain attenuate slowly. The distribution of the field in the metal is described by formulas (4.21)–(4.24), in which $\cos(n\pi/2)$ must be replaced by $[\cos(n\pi/2)](1 + 2\omega/\Omega)$. The form of the surface-impedance resonance curve is determined near the maximum by the formula

$$Z = Z_0\frac{1}{2\pi}\int_0^{2\pi}\frac{dq}{(1-\sin q + w)^{1/4}}, \tag{7.8}$$

which is valid when $|w| < 1$. The nonresonant factor Z_0 is determined by (7.7). When $|\Delta\omega| \ll \varphi\Omega(D_0/\delta)^{1/2}$, the quantity $|w|$ is small, and the impedance Z is larger than Z_0 by a factor 1.4. Figure 11 shows the schematic form of the resonance curves. Their characteristic width $\Delta H/H \sim \varphi(D_0/\delta)^{1/2}$ is due to the scatter of the diameters, and not to the electron collisions.

Finally, in the angle interval

$$\frac{\delta}{D_0} < \varphi < \left(\frac{\delta}{D_0}\right)^{1/2} \tag{7.9}$$

the oscillating part of the conductivity $\sigma(k)$ is determined as before by one resonant term with $\omega \simeq n\Omega$, and the part of $\sigma(k)$ that depends smoothly on k is given by (5.34). In other words, the skin layer is formed by all the electrons (which are mostly nonresonant), and the bursts are produced by a small group of resonant particles with small p_H. The addition to the impedance is due to the partial return of the field from the first burst to the surface on the metal, and is of the form

$$Z - Z_0 = \frac{2^7}{\pi^2}\frac{\omega\delta_0^2}{(R\varphi c)^2}F\left(\frac{2\sqrt{2}\omega}{\varphi\Omega}\sqrt{\frac{\delta_0}{R}}\right), \tag{7.10}$$

$$Z_0 = \frac{16\pi}{3\sqrt{3}}\frac{\omega\delta_0}{c^2}\exp\left(-\frac{\pi i}{3}\right), \qquad \delta_0 = \left(\frac{c^2 l}{2\pi^2\omega\sigma_0}\right)^{1/3}. \tag{7.11}$$

The function

$$F(w) = \frac{1}{2\pi}\int_0^{\infty}\frac{dq}{q(q^3-i)}\int_0^{\infty}\frac{d\xi}{\xi}\sin q\xi^2\exp(i\xi w) \tag{7.12}$$

describes the form of the resonant peaks. Near resonance $|w| \ll 1$ and $F(w) \simeq \ln(1/w)$, i.e., the CR is logarithmic. When $\varphi > (\delta_0/D_0)^{1/2}$, the width of the maxima becomes larger than the distance between them and the CR vanishes (Fig. 12).

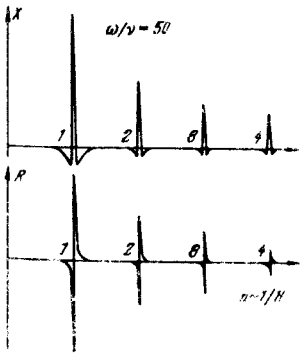

FIG. 10.

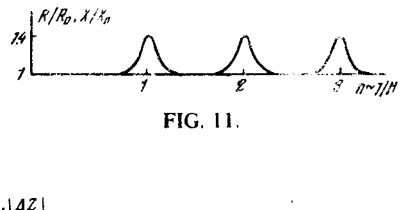

FIG. 11.

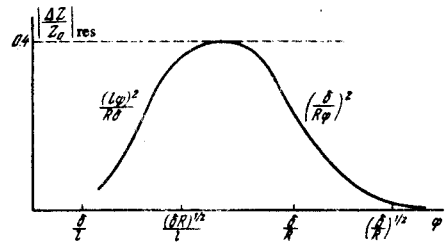

FIG. 12. Schematic form of the dependence of the relative amplitude of the resonance on the inclination angle φ.

Estimates of the amplitude in the corresponding region of angles are marked near the curves.

Inasmuch as in an inclined field the CR is due to AP of electromagnetic waves in the metal, the resonant values of the impedance have a maximum and not a minimum, corresponding to a larger transparency of the metal. The width and the form of the resonance curves is determined not by the dissipative processes (collision frequency ν), but by the scatter of the diameters of the electrons that produce the "chain" of trajectories.

If the electron dispersion is nonquadratic, the cyclotron frequency Ω depends on p_H. Near the central (extremal) cross section of the Fermi surface, the resonance condition

$$\omega = n\Omega_0 + \frac{1}{2} n\Omega_0'' p_H^2 + k\bar{v}_z(p_H) \qquad (7.13)$$

is satisfied by two groups of electrons, and not by one as in the case when $\Omega(p_H) = \text{const}$ (the prime denotes here differentiation with respect to p_H). It is shown in[23] that this leads to an appreciable decrease of the maximum amplitude of the peaks and of the resonant value of the impedance. In particular, in the angle region (4.18), the maximum value of ΔZ_{res} is only 3% of Z_0. This decrease of ΔZ_{res} compared with the case of quadratic dispersion is due to the fact that the skin layer is formed by both groups of the resonant electrons (7.13), whereas the peaks of the field and ΔZ_{res} are determined by one group in which the scatter of the diameters ΔD is small compared with δ. In all the remaining cases the deviation of the electron dispersion from quadratic does not play an important role.

It is of interest to compare the considered AP mechanism with the mechanism whereby a chain of trajectories is produced when $\varphi = 0$ in metals with nonquadratic dispersion law[4]. In the case investigated by Azbel', the selection of electrons by diameters is as a result of the CR itself. This selection mechanism is effective if (see Sec. 4.2) $R/\delta \ll \omega/\nu$. The theory developed above for CR in an inclined magnetic field is valid under the opposite condition, $R/\delta \gg \omega/\nu$. Consequently, the mechanism proposed in[23] for AP and CR in an inclined field is to a certain degree an alternative and a complement to the mechanism considered in[4].

Inversion of the CR peaks on the central sections of the Fermi surface following inclination of the magnetic field was observed in potassium[24], copper[25], silver[26], bismuth[27], and apparently in cadmium[28]. Figure 13a shows the experimental curves for copper.

7.2. Focusing of electrons from the vicinity of the limiting point and doubling of cyclotron resonances. The field peaks produced in a metal by the electrons of the limiting point also lead to interesting features of CR. This effect was first observed and correctly interpreted qualitative by Grimes et al.[29] in an investigation of CR in aluminum (Fig. 13b). It was later observed also in indium[30].

The phase of the field in the r-th peak at the instant t is

$$\omega t = \frac{2\pi r\omega}{\Omega_0} \qquad (r = 1, 2, \ldots),$$

where ωt—phase of the field on the surface. The electrons moving from inside the metal negotiate the distance from r-th peak to the surface within the same time $2\pi r/\Omega_0$. The phase difference between the external field and the peak field "returning" to the surface is obviously $4\pi r\omega/\Omega_0$. If $4\pi\omega/\Omega_0 = 2\pi n$, i.e., $\omega = n\Omega_0/2$, then the external field and the fields from all the peaks (with arbitrary r) are in phase. Consequently, a "doubling" of the resonant frequencies takes place ($\Omega_0 = 2\omega/n$).

The formulas obtained in Sec. 5.2 for the field distribution in the metal are valid also in the region of high frequencies $\omega \gg \nu$, but, unlike the low-frequency case, they contain an additional phase factor $\exp(2\pi i n\omega/\Omega)$. To determine the change of the surface impedance ΔZ of the half-space due to the AP in a metal, it is necessary to calculate $\Delta T(0)$ (see (5.21)). To this end it is necessary to take into account in (5.16) all the peaks in the volume of the metal. Since the diffuse scattering of the electrons by the surface of the metal does not play an important role and changes only a numerical factor on the order of unity in ΔZ, it is possible to neglect the θ-function in (5.16), and write $\Delta j_y(z)$ in the form

$$\Delta j_y(z) = \frac{2e^2}{(2\pi\hbar)^3 K_0} \sum_{n=1}^{\infty} \exp\left(-2\pi i n \frac{\nu - i\omega}{\Omega_0}\right) \iiint d\lambda \, d\varepsilon \, dp_H \times \left[E_y\left(z - nu_0 - \frac{1}{2} nu_0''\lambda^2 + \frac{1}{2}\varepsilon'' - \frac{1}{6} p_H^3\right) + E_y\left(z + nu_0 + \frac{1}{2} nu_0''\lambda^2 + \frac{1}{2}\varepsilon'' - \frac{1}{6} p_H^3\right)\right] \qquad (7.14)$$

Let us change to Fourier components. For $\delta_y(k)$ we obtain Eq. (3.13), in which

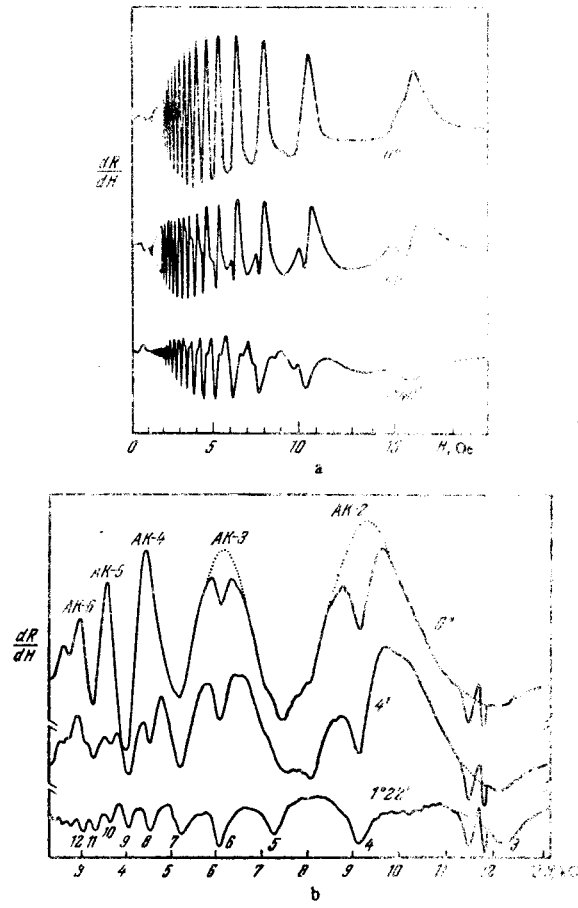

FIG. 13. a) CR in copper; $\mathbf{E} \perp \mathbf{H} \parallel [100]$. The [illegible] is indicated on the curves (from [25]). b) CR at the [illegible] aluminum; $Oz \parallel [100]$, $\mathbf{H} \parallel [1\bar{1}1]$ (from [29]).

$$\sigma_{yy}(k) = \sigma_0(k)\left[1 + \alpha \frac{4\sqrt{2}}{(ku_0)^{1/2}}\rho(ku_0)\right], \quad (7.15)$$

$$\rho(x) = \frac{1}{\sqrt{\pi}}\sum_{n=1}^{\infty} n^{-1/2}\cos\left(nx + \frac{\pi}{4}\right)\exp\left(-2\pi n\frac{\nu}{\omega}\right). \quad (7.16)$$

The function $\sigma_0(k)$ is given by formula (5.19) and α is given by (5.23). Substituting (7.15) in (3.18) we get

$$Z_{yy} \equiv Z = -8i\omega u_0 c^{-2}\int_0^{\infty}\frac{dqq}{q^3 - i\left(\frac{u_0}{\delta}\right)^3[1 + 4\sqrt{2}\,\alpha q^{-1/2}\rho(q)]}. \quad (7.17)$$

(δ is determined by formula (5.21)). In the integral with respect to q, at large values of u_0/δ, the principal role is played by large $q \sim u_0/\delta$. Therefore the change of the impedance ΔZ can be obtained with the aid of a formal expansion of the integrand in (7.17) in powers of $\alpha\rho(q)$. The term linear in α (and in $\rho(q)$) is small, owing to the rapid oscillations of the function $\rho(q)$ at large values of q. Therefore

$$\Delta Z \equiv Z - Z_0 = i\frac{2^8\omega u_0^3\alpha^2}{c^2\delta^6}\int_0^{\infty}\frac{dq\rho^2(q)}{\left[q^3 - i\left(\frac{u_0}{\delta}\right)^3\right]^3}, \quad (7.18)$$

where Z_0 is given by (7.11). The main contribution to ΔZ is made by the nonoscillating part of the function $\rho^2(q)$, which is equal to

$$(2\pi)^{-1}\sum_{n=1}^{\infty} n^{-1}\exp\left(4\pi\frac{i\omega - \nu}{\Omega_0}n\right) = -(2\pi)^{-1}\ln\left[1 - \exp\left(-4\pi\frac{\nu - i\omega}{\Omega_0}\right)\right].$$

Consequently,

$$\Delta Z = |Z_0|\alpha^2\frac{80}{9\pi}\frac{\delta}{R\sin\varphi}\exp\left(\frac{5\pi i}{6}\right)\ln\left[1 - \exp\left(4\pi\frac{i\omega - \nu}{\Omega_0}\right)\right]. \quad (7.19)$$

Thus, the field peaks produced in a metal by the drift of electrons from the vicinity of the limiting point, lead to a logarithmic CR at frequencies $\omega = n\Omega_0/2$. Formula (7.19) describes the form of the resonance lines. Just as in the case of CR on central sections, the resonance lines are inverted. At resonance, the amplitudes of $\partial R/\partial h$ and $\partial X/\partial H$ do not depend on the number. The width of the resonances is determined by the electron collisions.

In the presence of effective electrons with extremal displacement during the period, such a CR should also be observed at inclination angles on the order of unity.

8. Connection Between the Trajectory Type of Anomalous Penetration of the Field Into a Metal and Weakly Damped Electromagnetic Waves

The phenomena of field AP of the trajectory type and of weakly damped electromagnetic waves in metals are closely related and are transformed into each other when the frequency or the magnetic field H is changed. This connection is most clearly manifest in those cases when the natural oscillations in the metal have a discrete frequency spectrum. The skin layer can be regarded as a source generating oscillations with all wave numbers, but of a single frequency ω. In the case of AP of the trajectory type, an in-phase excitation of all the proper wavelengths takes place, and the interference between them leads to the peaks. This is nonresonant excitation. On the other hand, if the frequencies of the external field and one of the natural frequencies coincide, then resonance occurs and a traveling weakly-damped wave is excited in the metal in addition to the peaks.

Such a picture can take place, for example, in the presence of a chain of trajectories in an inclined magnetic field. As shown in[31], in alkali metals there should exist waves with discrete spectra of the frequencies

$$\omega_n = \frac{(8\pi)^{1/2}}{3}\left(\frac{H^2}{8\pi N\varepsilon_F}\right)\varphi\Omega(k_nR)^{3/2} \ll \Omega \quad (8.1)$$

and of the wave numbers k_n, which are determined from the equation $\sigma_{xx}(k_n) \sim 1 - \sin k_nD_0 = 0$ (cf. (4.19)).

A similar situation should occur also in CR. In metals with a nonquadratic electron dispersion in the direct vicinity of the CR, when $|(\omega/n) - \Omega_0| \ll \nu$, there is a system of peaks[4] (see Sec. 4.2), and if $|(\omega/n) - \Omega_0| \gg \nu$ these peaks are transformed into weakly damped waves[32].

Notice should also be taken of the connection between the field AP due to the focusing of the ineffective electrons (see Sec. 6) with helical or magnetohydrodynamic waves. These waves exist in strong magnetic fields, when $R \ll \delta$. With decreasing magnetic field, at a certain value of $H = H_e$, there appears a group of resonant electrons that absorb strongly the energy of the wave (Landau damping). The field H_e is determined by the equation ($\mathbf{H} \parallel Oz$)

$$\frac{eH_e}{mc} = k_w(H_e)v_{H\max} - \omega, \quad (8.2)$$

where $v_{H\max}$ — maximum velocity of the electrons along the field on the Fermi surface, and k_w — wave vector of weakly damped wave. When $H > H_e$, the electrons responsible for the absorption are missing and the damping of the wave is small, whereas in the region $H \ll H_e$ the collective oscillations become strongly damped.* On the other hand, when $H \ll H_e$ the motion of the ineffective electrons leads to AP of the trajectory type (see Sec. 6). Consequently, the field H_e serves as the boundary between the regions of existence of field AP of the trajectory type and of weakly damped electromagnetic waves.

II. EXPERIMENT (RADIO-FREQUENCY SIZE EFFECTS)

9. Methods of Experimental Observation of Field Anomalous Penetration of the Trajectory Type in a Metal

9.1. Nature of radio-frequency size effects. The possibilities and methods of experimentally observing field AP in a metal are determined by the relation between the frequency ω of the external field and the collision frequency ν. At high frequencies the field AP in a metal can be observed by measuring the impedance of the half-space, since it leads to CR. At low frequencies (3.19), the field AP gives only the half-space impedance component that varies monotonically with H, and this component cannot be separated in practice. Consequently, the only presently available experimental possibility of studying AP at low frequencies is connected with the radio-frequency size effects, which we shall now discuss.

Assume that an electromagnetic wave is incident on one side of a plane-parallel metallic plate of thickness

*The presence of an "absorption edge" is also called "cyclotron resonance shifted as a result of the Doppler effect"[33].

$d \gg \delta$. Only part of the system of peaks is contained in the plate. Their number depends on the thickness d and on the magnetic field H. By varying H, we can satisfy the relation

$$d = nD_{ext} \quad \text{or} \quad d = u_{n ext} \tag{9.1}$$

and by the same token "extract" one of the peaks through the opposite side of the plate. The electromagnetic field which appears there is radiated in space and can be observed. With further variation of H, the conditions (9.1) are violated and the plate ceases to be transparent to the electromagnetic field. Thus, the electric characteristics of the plate vary periodically as a function of the magnetic field. This is precisely the radio-frequency size effect (SE).

Generally speaking, the SE may or may not be connected with the field AP. In a sufficiently strong magnetic field parallel to the surface of the metal, the electrons return many times to the skin layer. When H is decreased, the maximum diameter of the trajectories increases and at a certain value $H = H_1$ it coincides with the thickness of the plate. Owing to the diffuse scattering of the electrons from the boundaries of the sample, such trajectories are "cut off"; their contribution to the current turns out to be small compared with the contribution from the electrons that are not scattered by the surface of the plate and do not return many times to the skin layer. When $H = H_1$, a singularity appears on the plot of the impedance against the field; the character of this singularity depends on the form of the extremal electron trajectories.

This phenomenon was first predicted by one of the authors[34] and observed experimentally by Khaĭkin[35] in experiments on CR in single-crystal plates of tin 1 mm thick (Fig. 14). On going over to higher CR numbers, the dimensions of the trajectories D increase. At $H < H_1$ (equal to 70 Oe) the resonant trajectories are no longer contained in the plate and the CR vanishes. The CR cutoff was observed subsequently also in other metals[36,37].

The same cutoff effect is obviously possible also in the region of low frequencies (3.19)[38,39]. The phase of the alternating field in the skin layer remains unchanged for each passage of the electron through the skin layer. The cutoff SE in the case of low frequencies has the form of an isolated peak on the plot of the impedance of the plate against H (see Figs. 15 and 16 below). Recently this SE became an important method of investigating the Fermi surfaces of conduction electrons in metals[5,39].

9.2. Methods of exciting the electromagnetic field in the plate. The metallic plate can be oriented in different manners relative to the source and the receiver of the electromagnetic field. This governs the character of the measured quantities. The plate can be oriented such that the wave is incident on it only on one side, and the reflected signal is measured. At high frequencies, such an experimental scheme can be realized by letting the sample serve as the wall of a resonator, and at low frequencies, by locating the sample near the end of an inductance coil perpendicular to its axis. In such experiments one measures the quantity

$$Z_d = 4\pi i\omega c^{-2} \frac{E(0)}{E'(0)}. \tag{9.2}$$

When the experiment is so performed, it is most convenient to observe the cutoff SE, since the second side of the plate, z = d, serves only as a "barrier" for the electron trajectories. Indeed, as shown in[34], the change of the plate impedance $Z_d(H)$ due to the "cutoff" of the electrons with extremal diameter D_{ext} is given by the formula

$$\frac{Z_d(H) - Z_\infty(H)}{Z_\infty(H)} = a_1 \left(1 - \frac{d^2}{D_{ext}^2}\right)^{1/2} \quad (d < D_{ext}). \tag{9.3}$$

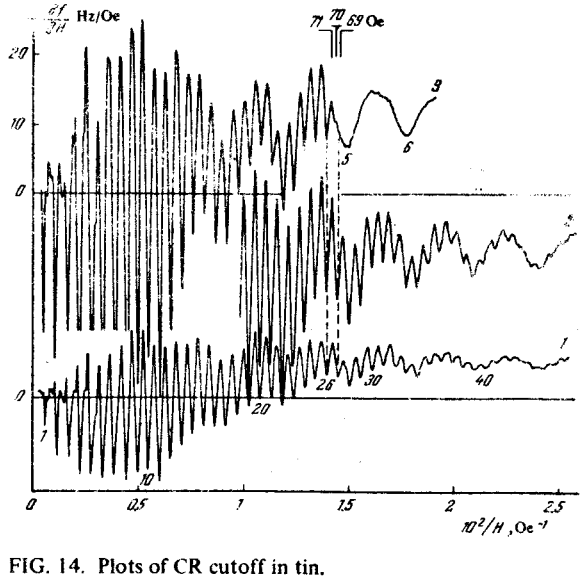

FIG. 14. Plots of CR cutoff in tin.

Oz || [100], E || [010], H || [001], frequency $f \simeq 10^{10}$ Hz, T = 3.75°K. Curves 1 and 2 – d = 2 mm, curve 3 – d = 1 mm. Curve 2 – part of curve 1 plotted with a larger magnification. The figures along the curves denote the number of the CR (from [35]).

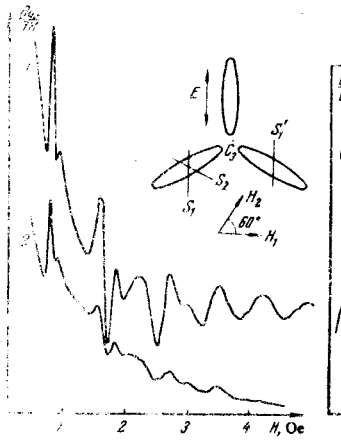

FIG. 15. Plots of the SE in bismuth at different directions of the magnetic field in the plane of the sample.

Oz || C_3, d = 1 mm, frequency f = 12 MHz, T = 1.8°K. The upper figure shows the arrangement of the electron ellipsoids and the polarization of the electric field. The indices of the vector H and of the extremal sections S and S' correspond to the numbers of the

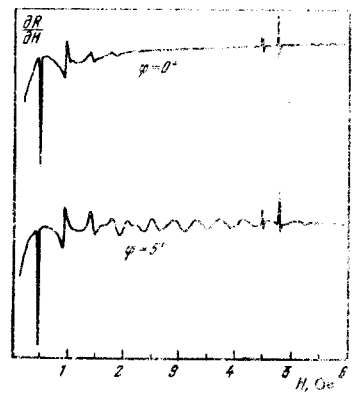

FIG. 16. Plots of the SE in rubidium.

d = 0.19 mm, frequency 19.5 MHz, T = 1.4°K, E ⊥ H. The peaks near 4.5 kOe represent a partly saturated NMR signal from protons and fluorine nuclei (from [44])

where a_1 is a constant on the order of unity (for a Fermi sphere, $a_1 = 4/3\pi$). The derivative of the impedance with respect to H (all the experiments described below consisted of measurements of the derivative) has a singularity of the type $(1 - d^2/D_{ext}^2)^{-1/2}$. The reason why $\partial Z/\partial H$ becomes infinite at $d = D_{ext}$ is that no account was taken in (9.3) of the smearing of the singularity as a result of the inhomogeneity of the field in the skin layer. It is quite obvious (as is also confirmed by exact calculation[40]) that the smearing of the singularity as a result of the finite skin-layer thickness δ leads to the estimate

$$\left|\frac{H}{Z}\frac{\partial Z}{\partial H}\right|_{max} \sim \left(\frac{d}{\delta}\right)^{1/2}. \tag{9.4}$$

On the other hand, the impedance (9.2) changes as a result of the AP of the field in the metal. In order to estimate the contribution made to Z_d by the field AP effects, we write down Maxwell's equations

$$k^2\mathcal{E}(k) - 2ik\mathcal{E}(0) - 2E'(d)\,k\sin kd - 2E'(d)\cos kd = 4\pi i\omega c^{-2}\sigma(k)\mathcal{E}(k). \tag{9.5}$$

(Continuation of the field $E(-z) = E(z)$, $E(z) = 0$ when $|z| > d$.) We neglect the influence of the finite thickness of the plate on the conductivity $\sigma(k)$. The term with $E'(d)$ in (9.5) can be disregarded, since it follows from the boundary condition at $z = d$ that $cE'(d) = -i\omega E(d)$. Consequently

$$-\frac{\pi}{2}\frac{E(0)}{E'(0)} = T(0) + \frac{E(d)}{E'(0)}\frac{\partial}{\partial d}T(d). \tag{9.6}$$

Substituting here in lieu of $E(d)/E'(0)$ the quantity $-2T(d)/\pi$, we obtain

$$\frac{Z_d - Z_\infty}{Z_\infty} = -\frac{4}{\pi^2 T(0)}\frac{\partial}{\partial d}T^2(d). \tag{9.7}$$

Thus, the change of the impedance of the plate due to the field AP is proportional, in the case of unilateral excitation, to $T^2(d)$ and not to $T(d)$ in the first power. This is connected with the fact that the field peak emerges to the surface $z = 0$ after "reflection" from the second side of the plate. Therefore the change of the derivative of the impedance from even the first peak is smaller by a factor $(d/\delta)^{1/2}$ than from the cutoff SE.

The experiment can be performed differently, namely, by irradiating the plate on one side and measuring the electromagnetic field on the other[41,42]. The measured signal is proportional to

$$\frac{E(d)}{E'(0)} \sim -2\pi^{-1}T(d), \tag{9.8}$$

i.e., to the first power of the function $T(d)$. In this case the SE is due to the field AP in the sample, and the cutoff effect plays no role.

Finally, if the sample is placed inside a resonant cavity[43] or else inside an inductance coil[38], two-sided symmetrical excitation of the plate is possible, with $H(0) = H(d)$ and $E(d) = -E(0)$. In this case each side of the plate is simultaneously a transmitter and a receiver, thus ensuring the possibility of observing all the known SE, including the cutoff effect. At low frequencies, this is precisely the excitation method employed. The coil with the sample serve as part of the tank circuit of a radio-frequency oscillator. The measured quantities—the change of the natural frequency of the tank circuit $f = \omega/2\pi$ and of its Q—depend on the depth of penetration of the alternating magnetic field in the plate

$$\Delta_\omega \sim \int_0^d \mathcal{H}_\omega^{(1)}(z)\,dz \sim \int_0^d H_\omega^{(1)}(z)\,dz, \tag{9.9}$$

where $H_\omega^{(1)}(z)$ is that part of the alternating magnetic field inside the metal, which is due to excitation of the plate from one side. Using Maxwell's equation $c\,\mathrm{curl}\,\mathbf{E}^{(1)} = i\omega\mathbf{H}_\omega^{(1)}$, we can rewrite (9.9) in the form

$$\delta_d = \frac{-2[E^{(1)}(0) - E^{(1)}(d)]}{E^{(1)'}(0)}. \tag{9.10}$$

Here $E^{(1)}(d)$ is the electric field on the second side of the plate, due to the AP of the field in the metal. On the other hand, the term with $E^{(1)}(0)$ describes the cutoff SE. From a comparison of (9.3) with (9.8) it follows that for closed orbits and for $d = D_{ext}$ the contributions to δ_d from the cutoff effects and from AP are of the same order of magnitude.

Let us define the impedance Z of the plate, in the case of two-sided excitation, by means of a formula similar to (1.2):

$$Z = -4\pi i\omega c^{-2}\Delta_\omega. \tag{9.11}$$

Using (3.14) and (9.10) we can finally rewrite (9.11) in the form (we omit the vector indices)

$$Z = 16i\omega c^{-2}[T(d) - 2(0)]. \tag{9.12}$$

We have tacitly assumed above that the field distribution in the plate coincides with the field distribution in the half-space. This is true only when the amplitude of the peak is much smaller than the field in the skin layer and the multiple reflection and interference of the waves in the plate can be neglected. In all the presently known experiments this condition is satisfied.

10. Experimental Investigation of Anomalous Penetration in a Metal with the Aid of Size Effects

All the experiments described below were performed in the frequency range 1 – 20 MHz with two-sided excitation of the plates. We discuss only those SE which are connected with the trajectory type field AP in the metal.

The amplitude of the SE lines is maximal when the incident-wave electric vector is polarized along the direction of the electron velocity in the effective point of the extremal trajectory. This makes it possible to separate experimentally certain SE from others.

10.1. Size effect on trajectory chains. Figures 15 and 16 show plots of the quantities $\partial\omega/\partial H \sim -\partial^2\Delta/\partial H^2$ and $\partial R/\partial H$ as functions of H for bismuth[43] and rubidium[44]. (The experimental conditions are indicated in the figure captions.) To identify the SE it is sufficient to verify that the position of the observed lines does not depend on the frequency and changes in inverse proportion to d. Indeed, the lines are located in those places where the condition (9.1) is satisfied. The formula for the position of the lines of SE from a chain of trajectories consisting of n links is

$$H_n = n\frac{2pc}{ed}, \tag{10.1}$$

where 2p is the extremal dimension of the orbit in the $z \times H$ direction. As seen from the figures, the interval of fields in which the SE lines are observed is not the same in rubidium and bismuth, thus reflecting the difference in the dimensions of the Fermi surfaces of these metals.

From the point of view of theory, the chain of trajectories in bismuth gives a "rapidly damped" system of peaks. The damping coefficient a (see (4.16)) is different for the two curves of Fig. 15. As is well known, the Fermi surface of bismuth consists of three electron "ellipsoids" and one "hole" surface. At a field direction H_1 (curve 1), the production of the system of peaks is due to two electron Fermi surfaces, and its "spreading" is due to the hole surface and the third electron "ellipsoid." At the field direction H_2 (curve 2), only one electron ellipsoid takes part in the formation of the system of peaks, whereas all the remaining carriers are responsible for the "spreading" of the peaks. Therefore at the field direction H_2 the value of a is smaller and the lines decrease more rapidly.

When investigating the intensities of the SE lines, it must also be borne in mind that D changes from number to number: $D(n) = d/n$ and $a^n \sim (n\delta/d)^{n/2}$. In addition, as already noted in Sec. 9.2, the intensity of the first line is determined not only by the AP, but also by the cutoff effect. Therefore a comparison with theory should be carried out using lines with $n \geq 2$, but their low intensity usually raises difficulties.

As indicated in Sec. 4.2, the attenuation of the peaks should decrease when the vector H is inclined, owing to the more efficient selection of electrons with a definite diameter D_0. This theoretical conclusion is confirmed by the curves of Fig. 16. They demonstrate the presence of a weakly damped chain of trajectories in a metal with a spherical Fermi surface. From the relative width of the line on the upper curve it is possible to estimate that $\delta/d \approx 0.1$. The inequalities (4.19), which represent the condition for weak damping of the peaks in the metal, are transformed into

$$0.1\left(\frac{\delta}{D}\right)^{1/2} \ll \varphi \ll 0.1n \qquad (n = 1, 2, 3 \ldots).$$

For the lower curve ($\varphi = 5^\circ \simeq 0.1$), these conditions are apparently satisfied for lines with numbers $n \geq 3$. It is precisely these lines which increase rapidly compared with the lines of the upper curve ($\varphi \sim 0$). It is interesting to note that the efficiency of the selection is retained also when $\delta \sim D(n \gtrsim 7)$, when individual peaks merge together and go over into a harmonic distribution of the alternating field in space.

The presence of several extremal diameters D_i increases the damping of the bursts and at the same time leads to the appearance of "secondary" peaks at depths $z = \Sigma n_i D_i$, i.e., the chain consists of "links" of different diameter. An example of a line due to such a chain is found in Fig. 21 below.

It is of interest to trace the variations of the positions of the SE lines from close trajectories when the magnetic field is inclined[45]. Their shift reflects the change of the depth of the location of the peaks with increasing angle φ: the line shift in the direction of the stronger fields denotes that the peak shifts deeper into the metal, and a line shift in the direction of weaker fields is evidence of a shift of the peak to the surface.

In metals with nonspherical Fermi surface, the closed trajectory usually does not lie in a plane perpendicular to H. Therefore the displacement of the electron along the field during the half-cycle when it moves from the surface of the metal to the peak can be different from zero. When $\varphi \neq 0$ there appears a projection of this displacement along the z axis. In calculating the position of the peak (or of the SE line), it is necessary to take into account the velocity component v_H, which does not enter in the vector equation (2.1). Let us consider, for example, a cylindrical Fermi surface with an axis $P \perp Oz$. Let the vector H be inclined in the (z, P) plane. The plane of the trajectory does not rotate when the field is inclined, and the dimension of the trajectory increases and is determined by the projection of the vector H on the cylinder axis. It is easy to show that the depth at which the burst is located is equal to

$$D_n(\varphi) = D_n(0)\cos\varphi, \qquad D_n(0) = n\left(\frac{2pc}{eH}\right). \tag{10.2}$$

The dependence of the position of the SE line on φ is given by

$$H_n(\varphi) = H_n(0)\sec\varphi, \tag{10.3}$$

where $H_n(0)$ is determined by formula (10.1). At small values of φ the line shift is $\Delta H \sim \varphi^2$.

A linear dependence of the shift on the angle φ is also possible. For example, in the case of a cylinder, the axis P of which is inclined to the surface at an angle $\varkappa$, we have following inclination of the field in the (z, P) plane

$$H_n(\varphi) = H_n(0)\frac{\cos\varkappa}{\cos(\varkappa-\varphi)} \approx H_n(0)(1-\varphi\operatorname{tg}\varkappa). \tag{10.4}$$

The quadratic (10.3) and linear (10.4) SE line shifts were observed experimentally in tin and in indium.

10.2. Size effect in inclined field in a metal with a spherical Fermi surface. In the study of the SE in potassium, Koch and Wagner[46] observed that the SE lines of the electrons of the central section of the Fermi surface shift towards stronger fields with increasing angle φ (Fig. 17). At the same time, z (the projection of the central diameter) decreases like cos φ in the cutoff field H_1. An explanation of this apparent contradiction can be found in Fig. 5. Owing to the presence of an extremum on the $u_1^{(1)}(p_H)$ curve, the peaks of the field and the SE are due to electrons with $u_{1\,ext}^{(1)}$, and not with $p_H = 0$. Using formula (5.4), we can show that the inequality $u_{1\,ext}^{(1)} \simeq D_0$ is always satisfied. In the case of small φ we have $u_{1\,ext}^{(1)} \simeq D_0(1 + 0.75\varphi^2)$. From the plots of $u_1^{(1)}$ it follows also that the SE should have a maximum intensity at $\varphi \cong 25^\circ$. This conclusion was also confirmed by experiment[46].

In[46] they observed also SE lines connected with extrema of the displacement $u_1^{(1)}$ near the boundary section of the Fermi surface. They confirm the conclusions of Sec. 5.3 that field peaks exist in a metal at large inclination angles φ.

10.3. Size effect due to the drift motion of the electrons inside the metal. We start with a discussion of

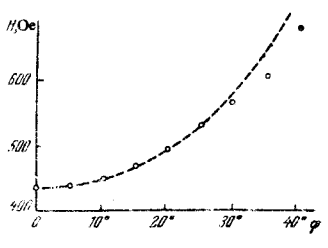

FIG. 17. Shift of SE lines in potassium with increasing inclination of the magnetic field.
Dashed – the function $H(\varphi) = H(0)/\cos^2\varphi$ (from [46]).

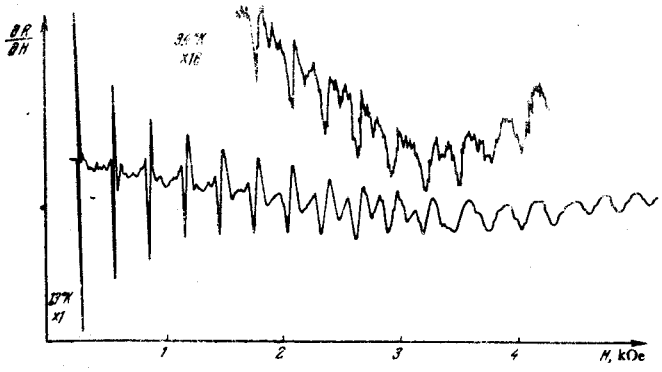

FIG. 18. Plot of SE at the limiting point in indium
Oz || [011], E || [111], $\varphi = 7°15'$, d = 0.3 mm, frequency f = 1.6 MHz. The upper curve was plotted with the gain increased 16 times.

the experimental data on the SE from elliptic limiting points. The velocity of the electrons at these points is parallel to the vector H and therefore the amplitude of the SE is maximal when the current j is polarized along the projection of the vector H on the surface of the metal (the y axis). A sample plot of this SE in indium is shown in Fig. 18[47]. It is easily distinguished from the other SE by the strong dependence of the period of ΔH on the inclination angle φ

$$\Delta H = \frac{2\pi c}{ed} K_0^{-1/2} \sin\varphi. \qquad (10.5)$$

According to formulas (9.12), (5.19), and (5.22) we have

$$\frac{\partial z}{\partial H} \sim -iC_0 H^{n} \exp\left(-\frac{d}{l_{0\varphi}}\right) \Psi_1\left(\frac{d - nu_0}{\delta}\right),$$
$$C_0 = 16\alpha\omega c^{-3} (8\pi^{-3}\delta d)^{1/2}, \quad n = \left[\frac{d}{u_0}\right]. \qquad (10.6)$$

The decrease of the amplitude of $\partial Z/\partial H$ with increasing number (~ 1/H) is due to the increase of the absolute line width $\sim H$. The amplitude of the field E in the peaks as such does not depend on the number, since the path length $d - nu_0$ remains unchanged (see (5.22)).

The dependence of the line amplitude for indium agrees well with (10.6). No such agreement was observed in the experiments with tin[11]. It is possible that the observed difference is connected with the field dependence of the effective frequency $\nu_{e,ph}$ of the electron-phonon collisions[48].

With increasing angle φ, the SE due to the limiting point goes over smoothly into the SE due to the electrons at the boundary section (see Sec. 5.3). The formula (10.5) for the period of ΔH then goes over smoothly into

$$\Delta H = \frac{\pi c}{ed} |m\bar{v}_H|_{\text{lim}} \sin 2\varphi. \qquad (10.7)$$

The SE from the boundary section was observed in[46], but so far the transition from (10.5) to (10.7) has not been traced directly.

All the SE considered above could actually be interpreted in terms of the model of a metal with a spherical Fermi surface. In a metal with a complex Fermi surface, there appear a number of specific possibilities for field AP and for SE (Secs. 5.2 and 5.4).

The anomalous penetration of the field as a result of the drift of the effective electrons on open orbits at $\varphi = 0$[11] is illustrated by the plots of Fig. 19. The presence of intermediate lines offers evidence of the complicated shape of the trajectories and of the existence of an additional sequence of points $u_n^{(1)}$ (5.2). The fundamental period is determined, in accordance with (5.6), by the formula

$$\Delta H = \frac{cb\cos\theta}{ed}. \qquad (10.8)$$

Characteristically, the lines were observed at all polarizations of the current j. This is connected with the presence of an entire layer of open orbits with identical period, which are equivalent from the point of view of the contribution to the effect. The directions of the electron velocities at the effective points depend in this case, probably, on p_H, forming a unique "fan" in the x, y plane.

Other interesting possibilities of the appearance of SE are connected with the existence of extremal helical trajectories of the type shown in Fig. 3. As indicated in Sec. 5.1, such a trajectory in an inclined magnetic field should lead to the appearance, generally speaking, of two sequences of peaks $z = u_n$ and $z = u_n^{(1)}$ in a semi-infinite metal. Each of the peaks can serve in turn as an initial skin layer for a secondary sequence at $2u_n^{(1)} + u_n$, $u_n^{(1)} + u_{n'}^{(1)}$, etc. These peaks result from a unique combination of two mechanisms of the field AP—along a chain of trajectories and as a result of the drift motion of the electrons. The amplitude of the primary sequences decreases with increasing number like $\exp(-\Lambda_n/l)$, where Λ_n is the length of the section of the trajectory from the surface of the metal to the corresponding burst (Fig. 20). The amplitude of the secondary sequence contains, besides the product of the amplitudes of the initial bursts, also a small "transfer coefficient" a (see Sec. 4.1).

In a parallel field we have $u_n = 0$, $u_n^{(1)} = D$, $u_n^{(1)} + u_{n'}^{(1)} = 2D$, ..., i.e., there exists the same system of peaks as that due to a chain of closed trajectories. Figure 20 shows schematically the location and the relative amplitudes of the peaks in a half-space in an inclined field. The same figure serves as a scheme for the arrangement of the SE lines as a function of the magnetic field, the only difference being that in a plate it is impossible

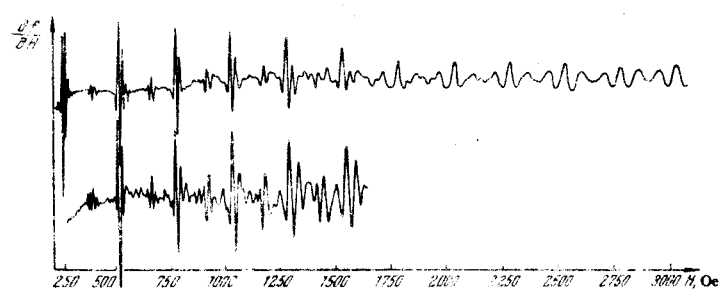

FIG. 19. Plot of SE on open trajectories in tin.
Oz || [001], H || [110], T = 2°K, frequency f = 3.2 MHz. Upper curve for E ⊥ H, lower – for E || H (from [11]).

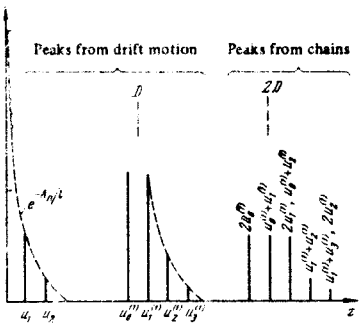

FIG. 20. Schematic distribution of the amplitudes of the peaks in an inclined field H in the presence of an extremal noncentral trajectory. The amplitude of the electric field at the surface is taken as unity.

to observe the SE due to peaks at a depth u_n, owing to the collisions between the electrons with the surface of the plate.

A similar picture was observed experimentally in indium[45], in which there exists a helical trajectory with extremal diameter $D \gg u$ (because of this all the quantities $u_n^{(1)}$ reach the extremum simultaneously). Figure 21 shows the splitting of the line D into the lines $u_0^{(1)}$ and $u_1^{(1)}$ when the field is inclined (the remaining lines are not seen, owing to the relatively small mean free path); the line at the depth 2D was split into three ($2u_0^{(1)}$, $u_0^{(1)} + u_1^{(1)}$, $2u_1^{(1)}$).

10.4. Size effect from electron trajectories with kinks. In experiments on SE it was established that in polyvalent metals (e.g., indium[45] and tin[50]) there exist trajectories with "kinks." We shall say that a trajectory has a "kink" if the electron velocity changes at a distance $\Delta z \ll \delta$ by an amount of the order of the velocity itself. Such a singularity leads to an anomaly in the distribution of the alternating field in the metal, and to corresponding SE lines which do not differ outwardly from other lines. The singularities in the distribution of the field due to the kinks on the trajectories lie between the peaks and are determined by the field amplitude at these points. According to (4.13), the relative magnitude of the observed singularity of the impedance is smaller by a factor $(D/\delta)^{1/2}$ than the amplitude of the succeeding peak. This is precisely the ratio observed in experiment[49].

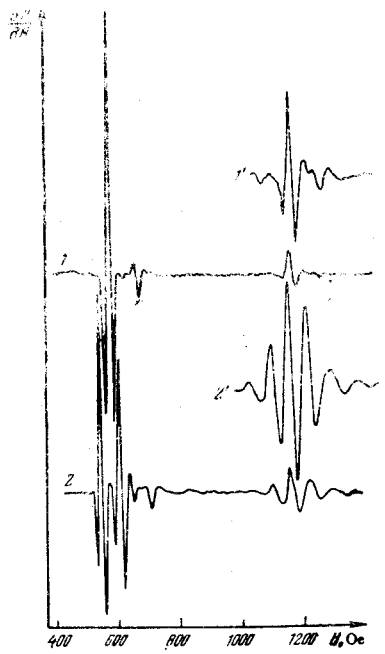

FIG. 21. Plots of SE in indium.
Oz || [001], E || [100], H ⊥ E, frequency f = 5 MHz, d = 0.3 mm. Curve 1 — $\varphi = 0$, curve 2 — $\varphi = 2.5°$. The right sides of the curves were plotted also with a gain increased by a factor of 5. The line marked with the asterisk is the SE from chains made of different links (from [45]).

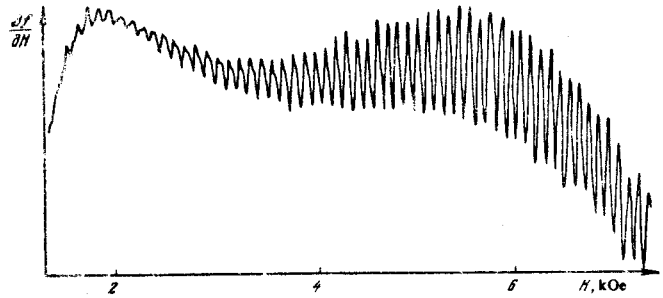

FIG. 22. Plot of SE in tin at $\varphi = 80°$.
Oz || [100], E || [010], T = 1.3°K, frequency f = 5.2 MHz.

10.5. Ineffective electrons. The harmonic component of the field distribution inside the metal, due to the drift of the ineffective electrons (Sec. 6), naturally leads to the appearance of a sinusoidal component of the surface impedance of the plate. The first two of the cases considered in Sec. 6 are realized when the magnetic field directions are close to the normal Oz. Experiments in a normal field were made on tin[15] (Fig. 22) and cadmium[52]. It is difficult to distinguish on these curves the oscillations due to the electrons of the limiting points and helical trajectories, because actually the only criterion is the relatively weak difference in the dependence of the amplitude of the oscillations on H. An analysis of this dependence is also made difficult by the fact that in the region of weak fields the modulating field may not penetrate fully into the sample.

It is therefore necessary to resort to indirect considerations: the shape of the Fermi surface, values obtained in other experiments for the curvature of the surface at the limiting points, the dependence of the period on the direction of H, etc. Such considerations indicate that all the hitherto observed oscillations in a normal field are connected with helical trajectories and not with limiting points. A role is possibly played here by the difference in the amplitudes by a factor $(d/u)^{1/2}$, which is noted in the theory.

Field AP into the metal was also observed in cadmium[22] as a result of the drift motion of the ineffective electrons on open periodic orbits, when the vector H is

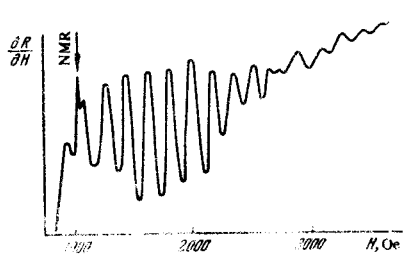

FIG. 23. Plot of SE in cadmium.
Oz || [11$\bar{2}$0], E || [10$\bar{1}$0], d = 0.4 mm, T = 1.7°K (from [22]).

parallel to the surface of the metal (see Sec. 6.3). Figure 23 shows a plot of the SE, illustrating this case of AP.

11. Line Shape of the Radio-frequency Size Effect

In the preceding section we actually discussed the experimental proof of the very existence of field AP in a metal of the trajectory type. The arrangements of the lines as a function of the magnetic field, which made it possible to classify the different types of SE, is a reflection of the "coarse" structure of the distribution of the field in a metal. To explain these "coarse" characteristics of AP and SE, it is actually sufficient to use the simple qualitative considerations based on the concept of "effectiveness" of the electrons and on the "extremum" principle.

The structure of the electromagnetic field inside the peaks, and the SE line shape, are more subtle characteristics of the AP phenomena, and their analysis requires the use of the rigorous theory developed in the first part of the present review. As shown in[12,40], the SE line shape is determined completely by the distribution of the electromagnetic field in the skin layer at the surface of the metal and by the shape of the electron trajectories near the effective points. Therefore a study of the line shape makes it possible to obtain direct information on the structure of the field in the skin layer and on the conduction-electron dispersion in metals. It must be emphasized that prior to the discovery of the SE there existed no direct method of investigating the distribution of the electromagnetic field in a metal. We note, first of all, that the SE line shape is not connected with any extraneous factors whatever. First, it is not affected by the degree of smoothness of the metal surface; when the samples are etched the line shape remains completely unchanged[49]. Consequently, the theoretical assumption that the boundary of the metal is a geometrically ideal plane is perfectly admissible from the point of view of a real experiment. Second, the wedgelike nature of the sample (the inhomogeneity of its thickness) leads to a splitting of the SE lines, and not to their smearing (Fig. 24). This is a unique manifestation of the "extremum" principle, but with respect to the thickness of the plate and not with respect to the electron trajectories.

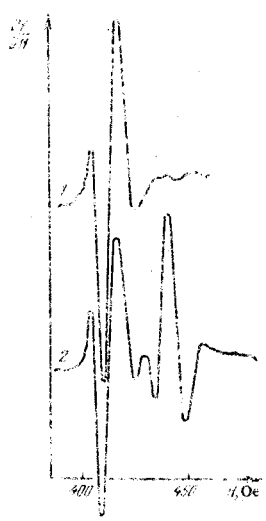

FIG. 24. Splitting of SE lines for a wedge-shaped indium sample. 1 – plane-parallel plate, d = 0.4 mm; 2 – wedge, $\Delta d/d = 7\%$.

The formulas obtained in Ch. I, in principle, describe correctly the distribution of the fields inside the peak and the law governing their decrease with increasing depth in the metal. However, owing to computational difficulties, the calculation was carried through to conclusion only in the case of field AP due to the electrons of the limiting point[12]. Using formula (10.6), it is possible to compare theory with experiment directly. Figure 25 shows the results of such a comparison for indium. The scale was chosen such as to ensure the best agreement between the theoretical and experimental curves on the right wings of the lines. As indicated in Sec. 5.2, the result of the calculations of the form of the burst and of the SE lines on the left edge depend strongly on the collisions of the electrons with the surface of the metal. The discrepancy between the theory and experiment in this region is due apparently to the fact that an approximate boundary condition (5.10) was used in the calculations (the trajectories of the focusing electrons were replaced by straight lines). It is probable that a more accurate analysis would decrease the value of the function $\Psi_1(x)$ at negative values of the argument.

It can thus be stated that the point corresponding to the condition $d = nu_0$ is located near the left edge of the SE line. This conclusion is confirmed by all the experimental data on the SE. It is valid not only for the SE from limiting points, but also for all the remaining types of SE. In a large number of cases, the arrangement of the lines was determined by the values of the parameters of the metal, which are well known from the theory or from other experiments (the period of the reciprocal lattice in tin[11], the dimension of the smallest semiaxis of the electron ellipsoid in bismuth[15], the diameter of the Fermi sphere in potassium[46], the Gaussian curvature at the limiting points in the [111] direction in indium[47] and aluminum[52]). In all these cases the points (9.1) corresponded to the left edge of the lines.

Consequently, in comparing experiment with theory

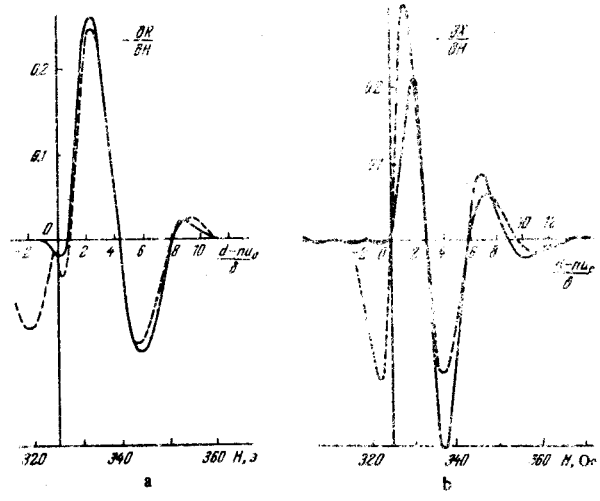

FIG. 25. Comparison of the experimental plots (solid) and theoretical (dashed) for SE lines of limiting points.

The ordinate scale pertains to the function Ψ (see Fig. 7). The experimental curves were obtained for indium; O_4 || [001], d = 0.3 mm, H || [111], $\varphi = 7°$, n = 1, T = 1.5°K, frequency f = 3 MHz.

it is possible to use the results of the calculations of the SE line shape without taking into account the collisions of the electrons with the surface of the metal (e.g., formulas (5.39) and (5.45)), discarding the part of the theoretical curve for $\delta < nu$.

Let us define the characteristic width Δ_H of the SE lines as the distance between two neighboring extrema of like sign. As seen from Figs. 7–9 and 25, the calculated width Δ_H is approximately equal to

$$\Delta_H \simeq (6\delta/d)\, H, \tag{11.1}$$

where

$$\delta = \frac{c^2}{4\pi\omega}\,\frac{|Z^2|}{X} = \frac{c^2}{3\pi\omega}\,X = \frac{c^2}{\sqrt{3}\,\pi\omega}\,R. \tag{11.2}$$

The experimentally obtained frequency dependence of the SE line width in indium[47], bismuth[5], and potassium[46], namely $\Delta_H \sim \omega^{-1/3}$, agrees with the theory of the anomalous skin effect. It is appropriate to mention here that the width Δ_H does not depend on the temperature (Fig. 18). This is due to the fact that in the anomalous skin effect the depth δ does not depend on the mean free path.

The absolute value of the characteristic depth of the skin layer δ can be obtained from the measured width of the SE lines with the aid of (11.1) and from independent measurements of the surface impedance by means of formula (11.2). The corresponding data for the three metals at 7.5 MHz are listed in the table together with the data on the mean free path[50]. The discrepancy, by a factor of 3, in the case of bismuth may be due to the insufficiently large value of the ratio $l/6\delta$.

	Sn	In	Bi
δ from ω, 10^{-5} cm	0.6	1.6	9
δ from H, 10^{-5} cm	1.8	2.8	150
l, cm	3.0	0.5	0.3

The SE lines can be observed with either the imaginary or the real part of Z. It is shown experimentally in[53] that the functions $\partial\mathcal{R}/\partial H$ and $\partial X/\partial H$ vary within the limits of the SE lines always in such a manner that the extrema of one of the functions approximately coincide with one of the positions of the fastest variation of the other. This regularity is a result of the structure of the field in the skin layer[40] (cf. the imaginary and real parts of T_0 (Fig. 6), Ψ_1, Ψ_2 (Fig. 7), Ψ_3 (Fig. 8), and Ψ_4 (Fig. 9)).

The distribution of the field in the skin layer is the fundamental but not the only factor of determining the SE line shape. Under the same conditions, lines of different shape are observed experimentally[39]. In the case of SE from the limiting point, an important role is played by a small section of the Fermi surface, which is well approximated by a second-order surface. Therefore the shape of the corresponding lines is accordingly well duplicated in different metals. On the other hand, when the closed trajectories are cut off, both the parameters of the extremal trajectory itself ($\partial v_Z/\partial\tau$ in the effective points) and the character of the extremum ($\partial^2 D/\partial p_H^2$) can change within a wide range[40]. Indeed, the line shape of the SE from closed trajectories is different for different extremal orbits. The entire aggregate of the experimental data offers evidence that the most significant factor governing the line shape is the time spent in the skin layer, characterized by the parameter $\partial v_Z/\partial\tau$[50].

Thus, the distribution of the field in the skin layer determines the main general features of the SE lines—the asymmetry with respect to the points (9.1), their width, the ratio of Re Z to Im Z, the character of the electron dispersion law determines the concrete line shape.

12. Applications of Size Effects

Radio-frequency size effects by now turned from being an object of study into a method of metal research. They are used most extensively to determine the form of the Fermi surface. The variety of information that can be obtained with their aid[5] is connected with the fact that the AP of the field in the metal is produced along electron trajectories of a great variety of types.

The cutoff of the closed trajectories determines the extremal dimensions of the Fermi surfaces and their anisotropy. A study of the behavior of the lines when the magnetic field is inclined can clarify the locations of the individual sections of the Fermi surface (see (10.3) and (10.4)). The limiting-point SE makes it possible to measure local values of the Gaussian curvature at elliptic limiting points. A study of the SE at large inclinations of the field to the surface makes it possible to observe trajectories with extremal displacement per period and to measure the values of $(\partial S/\partial p_H)_{ext}$. It is possible to prove with the aid of the SE the presence of orbits with kinks and of open orbits, and also to draw certain conclusions concerning their forms.

The most detailed studies made with the aid of the SE were those of the Fermi surfaces of tin[39,54], indium[47,49], and cadmium[22,51,55], and also gallium[57], tungsten[41], and molybdenum[56]. In particular, it is precisely the data on the SE which made it possible to determine the numerical values of the coefficients of the Fourier expansion of the pseudopotential in tin[55].

Another important application of the SE is the measurement of the mean free path l of individual groups of electrons on the Fermi surface. The possibility of measuring l is connected with the fact that the amplitude of the lines depends in most cases on l exponentially ($\sim \exp(-\Lambda/l)$, where Λ is the length of the path from one side of the plate of the other along the corresponding trajectory). In this respect, the limiting-point SE is particularly convenient, since variation of the angle φ results in a change in the path length $\Lambda = d/\sin\varphi$. The first such measurements were made in tin[11] for two limiting points. The mean free paths of two groups of electrons differ by a factor of 4, although the measurements were performed on a single sample. This method was used to measure also the dependence of the mean free path on the temperature in tin[48] and indium[47]. It turned out that $1/l(T) = 1/l(0) + CT^3$. The cubic temperature dependence offers evidence that the collision of electrons with even one phonon removes the electron from the focusing group. Therefore the quantity CT^3 is simply the probability of electron-phonon collision per

unit path. This fact agrees with the conclusions of the theory of the anomalous skin effect[7].

We note also one interesting radiospectroscopy application of the field AP in metals. Peercy and Walsh[44] succeeded in observing nuclear magnetic resonance in a bulky single crystal of rubidium, owing to the fact that the radio-frequency field penetrated along a trajectory chain through practically the entire sample. The variety of the already feasible applications gives grounds for hoping that the anomalous penetration of the field in a metal and the size effects will find wide applications in metal physics.

[1] G. E. Reuter, and E. H. Sondheimer, Proc. Roy. Soc. A195, 336 (1948).

[2] A. B. Pippard, Proc. Roy. Soc. A191, 385 (1947).

[3] É. A. Kaner and V. G. Skobov, Usp. Fiz. Nauk 89 367 (1966) [Sov. Phys.-Usp. 9, 480 (1967)].

[4] M. Ya. Azbel', Zh. Eksp. Teor. Fiz. 39, 400 (1960) [Sov. Phys.-JETP 12, 283 (1961)].

[5] V. F. Gantmakher, Progress in Low Temp. Phys. 5, 181 (1967).

[6] I. M. Lifshitz and M. I. Kaganov, Usp. Fiz. Nauk 69, 419 (1959) [Sov. Phys.-Usp. 2, 831 (1960)].

[7] M. Ya. Azbel' and É. A. Kaner, Zh. Eksp. Teor. Fiz. 32, 896 (1957) [Sov. Phys.-JETP 5, 730 (1957)]; Phys. Chem. Solids 6, 113 (1958).

[8] R. G. Chambers, Proc. Phys. Soc. A65, 458 (1952).

[9] É. A. Kaner, Zh. Eksp. Teor. Fiz. 34, 658 (1958) [Sov. Phys.-JETP 7, 454 (1958)].

[10] É. A. Kaner, ibid. 44, 1036 (1963) [17, 700 (1963)].

[11] V. F. Gantmakher and É. A. Kaner, ibid. 45, 1430 (1963) [18, 988 (1964)].

[12] É. A. Kaner, Physics 4, (1968).

[13] É. A. Kaner and V. L. Fal'ko, Zh. Eksp. Teor. Fiz. 49, 1895 (1965) [Sov. Phys.-JETP 22, 1294 (1966)].

[14] J. Heading, Introduction to Phase Integral Methods, Methuen, 1962.

[15] V. F. Gantmakher and É. A. Kaner, Zh. Eksp. Teor. Fiz. 48, 1572 (1965) [Sov. Phys.-JETP 21, 1053 (1965)].

[16] E. H. Sondheimer, Phys. Rev. 80, 400 (1950).

[17] V. L. Gurevich, Zh. Eksp. Teor. Fiz. 35, 668 (1958) [Sov. Phys.-JETP 8, 464 (1959)].

[18] T. Holstein and P. C. Siebenmann, Phys. Rev. 107, 1242 (1957).

[19] H. H. Zebouni, R. E. Hamburg, and H. T. Mackey, Phys. Rev. Lett. 11, 260 (1960).

[20] J. A. Munarin and J. A. Marcus, Paper at Ninth Internat. Conference on Low-Temperature Physics, USA, 1965.

[21] M. Ya. Azbel' and M. I. Kaganov, Dokl. Akad. Nauk SSSR 102, 49 (1955).

[22] A. A. Mar'yakhin and V. P. Naberezhnykh, ZhETF Pis. Red. 3, 205 (1966) [JETP Lett. 3, 130 (1966)].

[23] É. A. Kaner and A. Ya. Blank, Phys. Chem. Solids 28, 1735 (1967).

[24] C. C. Grimes and A. F. Kip, Phys. Rev. 132, 1991 (1963).

[25] J. F. Koch, R. A. Stradling, and A. F. Kip, Phys. Rev. A133, 240 (1964).

[26] D. G. Howard, Phys. Rev. 140, A1705 (1965).

[27] M. S. Khaĭkin and V. S. Édel'man (private communication).

[28] A. ... , T. G. Eck, and D. A. Zich, Phys. Rev. 142, 406 (1966).

[29] C. C. Grimes, A. F. Kip, F. M. Spong, R. A. Stradling, and P. Pincus, Phys. Rev. Lett. 11, 455 (1963); F. W. Spong, A. F. Kip, Phys. Rev. 137, A431 (1965).

[30] R. T. Mina and M. S. Khaĭkin, ZhETF Pis. Red. 1, (2), 34 (1965) [JETP Lett. 1, 60 (1965)].

[31] É. A. Kaner and V. G. Skobov, Physics 2, 185 (1966).

[32] É. A. Kaner and V. G. Skobov, Fiz. Tverd. Tela 6, 1104 (1964) [Sov. Phys.-Solid State 6, 851 (1964)].

[33] J. Kirsch, and P. B. Miller, Phys. Rev. Lett. 9, 421 (1962).

[34] É. A. Kaner, Dokl. Akad. Nauk SSSR 119, 471 (1958) [Sov. Phys.-Dokl. 3, 314 (1958)].

[35] M. S. Khaĭkin, Zh. Eksp. Teor. Fiz. 41, 1773 (1961) [Sov. Phys.-JETP 14, 1260 (1962)]

[36] R. T. Mina and M. S. Khaĭkin, ibid. 48, 111 (1965) [21, 75 (1965)].

[37] M. S. Khaĭkin and V. S. Édel'man, ibid. 47, 878 (1964) [20, 587 (1965)].

[38] V. F. Gantmakher, ibid. 42, 1416 (1962) and 43, 345 (1962) [15, 982 (1962) and 16, 247 (1963)].

[39] V. F. Gantmakher, ibid. 44, 811 (1963) [17, 549 (1963)].

[40] É. A. Kaner and V. L. Fal'ko, ibid. 51, 586 (1966) [24, 392 (1967)].

[41] W. M. Walsh, Jr., and C. C. Grimes, Phys. Rev. Lett. 13, 523 (1964).

[42] R. B. Leurs and T. R. Garver, Phys. Rev. Lett. 12, 693 (1964).

[43] M. S. Khaĭkin, PTE No. 3, 95 (1961).

[44] P. S. Peercy, and W. M. Walsh, Jr., Phys. Rev. Lett. 17, 741 (1966).

[45] V. F. Gantmakher and I. P. Krylov, Zh. Eksp. Teor. Fiz. 47, 2111 (1964) [Sov. Phys.-JETP 20, 1418 (1965)].

[46] J. F. Koch and T. K. Wagner, Phys. Rev. 151, 467 (1966).

[47] I. P. Krylov and V. F. Gantmakher, Zh. Eksp. Teor. Fiz. 51, 740 (1966) [Sov. Phys.-JETP 24, 492 (1967)].

[48] V. F. Gantmakher and Yu. V. Sharvin, ibid. 48, 1077 (1965) [21, 720 (1965)].

[49] V. F. Gantmakher and I. P. Krylov, ibid. 49, 1054 (1965) [22, 734 (1966)].

[50] V. F. Gantmakher and I. P. Krylov, Paper at Tenth International Conference on Low Temperature Physics, Moscow, 1966.

[51] A. A. Mar'yakhin and V. P. Naberezhnykh, Zh. Eksp. Teor. Fiz. 52, 617 (1967) [Sov. Phys.-JETP 25, 403 (1967)]; Phys. Stat. Sol. 20, 737 (1967).

[52] J. F. Koch and T. K. Wagner, Bull. Amer. Phys. Soc. 11, 170 (1966).

[53] I. P. Krylov, ZhETF Pis. Red. 1 (4), 24 (1965) [JETP Lett. 1, 116 (1965)].

[54] V. F. Gantmakher, Zh. Eksp. Teor. Fiz. 46, 2028 (1964) [Sov. Phys.-JETP 19, 1338 (1964)].

[55] G. Weisz, Phys. Rev. 149, 504 (1966).

[56] R. G. Goodrich and R. C. Jones, Phys. Rev. 156, 745 (1967).

[57] A. Fucumoto and M. W. P. Strangberg, Phys. Rev. 155, 685 (1967).

[58] V. V. Boĭko, V. A. Gasparov, and I. G. Gverdtsiteli, ZhETF Pis. Red. 6, 737 (1967) [JETP Lett. 6, 212 (1967)].

Translated by J. G. Adashko